Xanthophyll carotenoids stabilise the association of cyanobacterial chlorophyll synthase with the LHC-like protein HliD

Matthew S. Proctor[a], Marek Pazderník[b,e], Philip J. Jackson[a,c], Jan Pilný[b], Elizabeth C. Martin[a], Mark J. Dickman[a,c], Daniel P. Canniffe[d], Matthew P. Johnson[a], C. Neil Hunter[a], Roman Sobotka[b,e] and Andrew Hitchcock[a]

[a]Department of Molecular Biology and Biotechnology, University of Sheffield, Sheffield S10 2TN, United Kingdom

[b]Institute of Microbiology of the Czech Academy of Sciences, Centre Algatech, 37981 Třeboň, Czech Republic

[c]Department of Chemical and Biological Engineering, University of Sheffield, Sheffield S1 3JD, United Kingdom

[d]Institute of Systems, Molecular & Integrative Biology, University of Liverpool, Liverpool L69 7ZB, United Kingdom

[e]Faculty of Science, University of South Bohemia, 37005 České Budějovice, Czech Republic

Authors for correspondence: Roman Sobotka (sobotka@alga.cz) and Andrew Hitchcock (a.hitchcock@sheffield.ac.uk)

Author ORCID IDs: 0000-0002-1484-850X (MSP); 0000-0001-9671-2472 (PJJ); 0000-0002-9236-0788 (MJD); 0000-0002-5022-0437 (DPC); 0000-0002-1663-0205 (MPJ); 0000-0003-2533-9783 (CNH); 0000-0001-5909-3879 (RS); 0000-0001-6572-434X (AH)

Abstract

Chlorophyll synthase (ChlG) catalyses a terminal reaction in the chlorophyll biosynthesis pathway, attachment of phytol or geranylgeraniol to the C17 propionate of chlorophyllide. Cyanobacterial ChlG forms a stable complex with high light-inducible protein D (HliD), a small single-helix protein homologous to the third transmembrane helix of plant light-harvesting complexes (LHCs). The ChlG-

HliD assembly binds chlorophyll, β-carotene, zeaxanthin and myxoxanthophyll and associates with the YidC insertase, most likely to facilitate incorporation of chlorophyll into translated photosystem apoproteins. HliD independently coordinates chlorophyll and β-carotene but the role of the xanthophylls, which appear to be exclusive to the ChlG-HliD assembly, is unclear. Here we generated mutants of *Synechocystis* sp. PCC 6803 lacking specific combinations of carotenoids or HliD in a background with FLAG- or His-tagged ChlG. Immunoprecipitation experiments and analysis of isolated membranes demonstrate that the absence of zeaxanthin and myxoxanthophyll significantly weakens the interaction between HliD and ChlG. ChlG alone does not bind carotenoids and accumulation of the chlorophyllide substrate in the absence of xanthophylls indicates that activity/stability of the 'naked' enzyme is perturbed. In contrast, the interaction of HliD with a second partner, the photosystem II assembly factor Ycf39, is preserved in the absence of xanthophylls. We propose that xanthophylls are required for the stable association of ChlG and HliD, acting as a 'molecular glue' at the lateral transmembrane interface between these proteins; roles for zeaxanthin and myxoxanthophyll in ChlG-HliD complexation are discussed, as well as the possible presence of similar complexes between LHC-like proteins and chlorophyll biosynthesis enzymes in plants.

Introduction

Carotenoids are isoprenoid pigments that are categorized into two main classes, xanthophylls, which contain oxygen, and carotenes, which do not. In chlorophototrophs carotenoids are important for light harvesting, photoprotection and structural stabilization of proteins and membranes (1, 2). For example, the trimeric photosystem I (PSI) from *Synechocystis* sp. PCC 6803 (hereafter *Synechocystis*) contains 72 carotenoids and is dependent upon β-carotene for trimerization (3-6). β-carotene is also a cofactor in photosystem II (PSII) and is required for its assembly (7, 8), is present in the cytochrome b_6f complex (9, 10) and photosynthetic complex I (11), and plays a role in the assembly of the phycobilisome antenna complex (5). In plants, xanthophylls play important roles in structural stabilization of light-harvesting complexes (LHCs), light harvesting and photoprotection, and act as lipid-soluble antioxidants (12-14). However, the role of xanthophylls in cyanobacteria, where they do not participate in light harvesting, is less obvious. There is a pool of free xanthophylls in cyanobacterial membranes that modulates membrane rigidity/fluidity (15, 16) and it is widely accepted that these pigments provide protection against photooxidative stress and reactive oxygen and nitrogen species, especially under high light conditions (17, 18). Although not integral components of either photosystem, xanthophylls stabilize oligomers of PSI and PSII (5, 19), while keto-xanthophylls are

specifically required for non-photochemical dissipation of excess energy by the orange carotenoid protein (20).

Chlorophyll (Chl) synthase (ChlG) is an integral thylakoid membrane protein that catalyses the addition of a geranylgeranyl or phytyl tail to the chlorophyllide (Chlide) macrocycle as one of the terminal steps of Chl biosynthesis (**Figure 1A**). In *Synechocystis*, tagged ChlG co-purifies with the carotenoids β-carotene, zeaxanthin and myxoxanthophyll in a pigment-protein complex also containing Chl, high light-inducible proteins (Hlips), the membrane insertase YidC and the PSII assembly factor Ycf39 (21, 22). ChlG binds tightly to HliD in a ChlG-HliD 'core', with YidC and Ycf39 present in sub-stoichiometric amounts (21). Hlips are single helix transmembrane pigment-binding proteins that are thought to be the ancestors of LHCs in eukaryotic phototrophs (23). *Synechocystis* contains four Hlips (HliA-D), which appear to be primarily involved in Chl biosynthesis/recycling and biogenesis and photoprotection of Chl-binding proteins (24), although their exact roles remain enigmatic. An Hlip domain is also found fused to the C-terminus of cyanobacterial and plant ferrochelatases (25). YidC assists in the integration of translated proteins into the membrane bilayer (26) and its association with ChlG is presumed to facilitate insertion of Chl molecules into newly synthesized Chl-binding proteins (21). The function of Ycf39 in the ChlG-HliD complex is unclear but it could play a regulatory role in re-modelling ChlG-Hlip assemblies in response to stress (27); Ycf39 and HliD interact in a separate complex that promotes the synthesis and assembly of the core PSII subunits D1 and D2 during exposure to high light (28), conditions under which Ycf39 dissociates from the ChlG complex (27) and HliD appears to be partially replaced by HliC (22).

The approximate molar ratio of pigments in the ChlG complex is Chl (6): zeaxanthin (2.1-2.7): β-carotene (1): myxoxanthophyll (0.6-1) (21, 22). HliD likely binds to ChlG as a dimer as the predicted structure of Hlips shows that they cannot bind pigments as monomers (29); purified HliD dimers bind 6 Chl *a* molecules and 2 β-carotenes (22). Ultrafast transient absorption spectroscopy indicates that one of the β-carotenes in the HliD adopts a 'twisted' configuration that can quench excited states of Chl, resulting in the safe dissipation of excitation energy as heat (22, 30, 31), leading to the suggestion that HliD photoprotects Chl-binding proteins and Chl-biosynthesis enzymes (24, 28, 30, 31). Given that neither isolated HliD nor the Ycf39-HliD complex binds xanthophylls (22; 28, 30), and specific removal of Ycf39 does not alter the pigment composition of the larger ChlG complex (27), the presence of zeaxanthin and myxoxanthophyll appears to be strictly dependent on interaction of ChlG and HliD, but their functional roles are unknown.

To investigate the requirement of xanthophylls in the ChlG-HliD complex, we generated a series of *Synechocystis* strains lacking either combinations of xanthophylls or HliD and performed

immunoprecipitations using tagged ChlG as bait. Our results demonstrate that zeaxanthin is required for stable formation of the ChlG-HliD complex, both *in vitro* and *in vivo*. ChlG alone does not co-purify with carotenoids and its function appears to be perturbed in the absence of the xanthophyll-mediated association with HliD. Possible roles of HliD in Chl trafficking and photosystem assembly/repair, and candidates which may perform analogous functions in higher phototrophs, are discussed.

Materials and methods

Growth of *Synechocystis* and strain generation

Synechocystis was grown at 30 °C with moderate light (30-50 µmol of photons $m^{-2}s^{-1}$) in BG11 medium (32) supplemented with 10 mM TES (Sigma Aldrich)-KOH pH 8.2 (BG11-TES). Liquid cultures were shaken at approximately 150 rpm. For growth on plates, BG11-TES was supplemented with 1.5% (w/v) agar and 0.3% (w/v) sodium thiosulphate. Antibiotics were included where appropriate (as detailed below). Cultures for purification of protein complexes were grown photoautotrophically with ~100 µmol photons $m^{-2}s^{-1}$ illumination in 8 L vessels which were mixed by bubbling with sterile air and maintained at 30 °C using a temperature coil connected to a thermostat-controlled circulating water bath.

All reported mutant strains were prepared in the *Synechocystis* WT-P (WT) substrain (33); the FLAG-*chlG* Δ*chlG* (FG/ΔG) strain generated in this background has been reported previously (27). To generate a strain producing 10xhistidine-tagged ChlG, the *Nde*I-*Bgl*II fragment encoding the 3xFLAG-tagged *chlG* in pPD-*N*FLAG::*chlG* (21) was replaced with sequence encoding 10xhistidine-tagged *chlG* (synthesised as a gBLOCK by Integrated DNA Technologies; see **Table S1** for sequence) and the resulting allele exchange construct (pAH97) was introduced into WT *Synechocystis* with selection and segregation on kanamycin, as detailed below. The zeocin resistance mutagenesis construct described by Chidgey et al. (21) was used to delete the native *chlG* gene (slr0056) from the His-*chlG* strain, generating the strain His-*chlG* Δ*chlG* (HG/ΔG).

To generate a *crtR* null mutant, a linear mutagenesis construct was generated by OLE-PCR to replace the central 555 bp of the 939 bp gene (sll1468) with an erythromycin resistance cassette by allele exchange. Similar constructs were generated to replace 568 bp of the 912 bp *cruF* gene (sll0814) with the *aadA* gene (streptomycin resistance) from pCDFDuet-1 (Novagen), 710 bp of the 1629 bp *crtO* gene (slr0088) with the chloramphenicol acetyl transferase (*cat*) from pACYC184 (NEB) or 722 bp of the 1185 bp *cruG* gene (sll1004) with *aadA*. The erythromycin resistance mutagenesis construct described by Xu et al. (34) was used to delete *hliD* (ssr1789). Linear DNA constructs were introduced

to *Synechocystis* by natural transformation and transformants were selected on BG11 agar with 7.5 μg ml^{-1} kanamycin, 7.5 μg ml^{-1} erythromycin, 5 μg ml^{-1} streptomycin, 12.5 μg ml^{-1} chloramphenicol or 2.5 μg ml^{-1} zeocin, as appropriate. Segregation of genome copies was achieved by sequential plating with increasing antibiotic concentration up to 20 μg ml^{-1} (for zeocin), 30 μg ml^{-1} (for erythromycin/streptomycin/kanamycin) and 50 μg ml^{-1} (for chloramphenicol) and was confirmed by colony PCR. All primers used to generate constructs and screen *Synechocystis* strains/mutants are provided in **Table S1**.

Purification of FLAG-tagged and His-tagged ChlG

FLAG-immunoprecipitations were performed as reported in our previous work (21, 27). *Synechocystis* cultures were grown to an OD_{750} of ~0.7-1.0, harvested by centrifugation (17 700x*g*, 4 °C, 20 min), resuspended in binding buffer (25 mM sodium phosphate pH 7.4, 10 mm $MgCl_2$ and 50 mm NaCl, 10% (w/v) glycerol and EDTA-free Protease Inhibitor [Roche]) and lysed in a Mini-Beadbeater-16. The lysed cells were collected from atop the glass beads and thylakoid membranes were pelleted by centrifugation (48 400x*g*, 4 °C, 30 min) and solubilised by incubation with 1.5% (w/v) n-dodecyl-β-D-maltoside (β-DDM; Anatrace) at 4 °C for 1 h. Following centrifugation (48 400x*g*, 4 °C, 30 min) to pellet insoluble debris, the solubilised thylakoid fraction (the supernatant) was diluted 2-fold and applied to a 300 μL anti-FLAG-M2 agarose (Sigma-Aldrich) column equilibrated in wash buffer (binding buffer with 0.04% (w/v) β-DDM). The resin was washed with 20 resin volumes of wash buffer to remove contaminating proteins and the FLAG-tagged bait protein and associated interaction partners were eluted in 400 μL of the same buffer containing 187.5 μg mL^{-1} 3xFLAG peptide (Sigma-Aldrich). The mixture was filtered through a 0.22 μm spin column (Sigma-Aldrich) to separate the resin from the eluted protein. Eluates were analysed immediately or stored at -80 °C.

For purification of His-ChlG (H.ChlG), solubilised thylakoids were applied three times to a Ni^{2+} NTA Agarose (Qiagen) immobilised metal affinity chromatography column that had been pre-equilibrated in binding buffer (as above) supplemented with 5 mM imidazole. Approximately 250 μL of resin was used per 8 L of cell culture from which the membrane fraction was isolated. The column was washed with 20 column volumes of binding buffer followed by washes with binding buffer containing progressively higher (20, 50 and 80 mM) imidazole concentrations, each containing 0.04% (w/v) β-DDM. H.ChlG was eluted by incubation of the resin with 400 μL of elution buffer (binding buffer containing 400 mM imidazole and 0.04% (w/v) β-DDM) for 1 h with gentle agitation at 4 °C before the solution was filtered through a 0.22 μm spin column, separating the resin from the eluted protein. Eluates were analysed immediately or stored at -80 °C.

Pigment analysis by reverse phase high performance liquid chromatography (RP-HPLC)

Pigments were extracted from cell pellets or FLAG-/His-eluates in 100% methanol and separated by RP-HPLC on an Agilent 1200 HPLC system using a Discovery HS C_{18} column (5 µm, 250 × 4.6 mm) according to the slightly modified method of that of Largarde and Vermaas (35) described in Proctor et al. (27). Absorbance was monitored at 450 nm and 665 nm and carotenoid species and Chl *a* were identified by their known absorption spectra (**Figure S1**) and retention time (**Figures S2** and reference 27).

Quantitative proteomic analysis

Proteins were extracted from the FLAG eluates by precipitation using a 2-D clean-up kit (GE Healthcare) and processed according to Hitchcock et al. (36) to generate tryptic peptides. Analysis was performed by nano-flow reverse phase chromatography coupled to a mass spectrometer using system parameters described by MacGregor-Chatwin et al. (37) with the exception that peptides were resolved with a 75 min gradient in this study. Proteins were identified and quantified using MaxQuant v.1.5.3.30 (38) to search a *Synechocystis* proteome database (http://genome.microbedb.jp/cyanobase/).

Protein electrophoresis and immunoblotting

Protein electrophoresis was performed as reported in our previous work (21, 27). Proteins in the FLAG- and His-eluates were separated by SDS-PAGE on Invitrogen 12% Bis–Tris NuPage gels (Thermo Fisher Scientific) and visualised by staining with Coomassie Brilliant Blue (Bio-Rad). For blue-native (BN)-PAGE, solubilised thylakoid membrane protein complexes, prepared as outlined above, were separated on 8-16% BN-gels (25) to resolve ChlG-HliD and Ycf39-HliD complexes. Protein complexes were further resolved by incubating the BN-gel strip in 2% (w/v) SDS and 1% (w/v) dithiothreitol for 30 min at room temperature followed by separation of individual protein components in the second dimension by SDS-PAGE in a denaturing 12 to 20% (w/v) polyacrylamide gel containing 7 M urea. For immunoblotting, proteins were transferred onto polyvinylidene fluoride membranes (Thermo Fisher Scientific) and incubated with specific primary antibodies against the 3xFLAG tag (Sigma-Aldrich), His_6-tag (Merck), HliD (Agrisera AS10-1615), ChlG (described in reference 21) or Ycf39 (21) followed by an appropriate secondary antibody (anti-rat for 3xFLAG, anti-mouse for His_6 and anti-rabbit for HliD, ChlG

and Ycf39) conjugated with horseradish peroxidase (Sigma-Aldrich) to allow detection using the WESTAR ETA C 2.0 chemiluminescent substrate (Cyanagen) with an Amersham Imager 600 (GE Healthcare).

Quantification of Chl and Chl precursors

Chl content was determined spectrophotometrically following extraction from cell pellets (from 1 mL of culture at $OD_{750} \approx 0.4$) with 100% methanol according to Porra et al. (39). Chl precursors were extracted from cell pellets (from 2 mL of culture at $OD_{750nm} \approx 0.4$) of WT and mutant *Synechocystis* strains (five biological replicates per strain) and analysed by RP-HPLC with two fluorescence detectors, as described previously (40). Equivalent peaks were integrated, summed, and calculated as a percentage of the WT values, which were set as 100%.

Results

Generation of strains with altered xanthophyll content

Photosynthetic carotenoids are C_{40} molecules synthesized from 8 C_5 isoprene units (41). *Synechocystis* accumulates four major carotenoid species, β-carotene, zeaxanthin, myxoxanthophyll and echinenone, and produces others in lesser amounts, including synechoxanthin, 3'-hydroxy-echinenone and β-cryptoxanthin (35, 42); the molecular structures of the major carotenoids are presented in **Figure 1B**. An overview of carotenoid biosynthesis from all-*trans*-lycopene, the last common precursor of all the mature carotenoids synthesized by *Synechocystis*, is given in **Figure S3**. Briefly, lycopene is cyclized at one or both of its ψ-ends producing γ-carotene (one β-ionone ring) or β-carotene (two β-rings); the myxoxanthophyll biosynthesis pathway branches from γ-carotene, whereas the other carotenoids are produced by modification of β-carotene. The carotenoid contents of WT *Synechocystis* and a strain containing an N-terminally 3xFLAG-tagged ChlG but lacking the native *chlG* (FG/ΔG) were analysed by RP-HPLC and the four expected major carotenoid species were identified (**Figure S2**).

Mutants unable to synthesize β-carotene display severe growth phenotypes because it is required for assembly of PSII (4, 7), but xanthophylls are dispensable for photoautotrophic growth under our low-stress laboratory conditions (35, 42, 43). Mutants lacking xanthophyll biosynthesis genes were generated in the WT and FG/ΔG strains (**Table 1**; **Figure S4**)**,** resulting in identical carotenoid deficiencies in both backgrounds (**Figure S2**; summarised in **Table 2**).

Deletion of the *crtR* gene, which encodes the β-carotene hydroxylase acting at the 3/3′ positions of the ionone rings of β-carotene (7), prevented biosynthesis of both zeaxanthin and myxoxanthophyll and resulted in the appearance of a new carotenoid species, previously identified as dehydroxy-myxoxanthophyll (myxoxanthophyll missing the hydroxyl group on the β-ring (35, 44)). It is not possible to generate a knockout strain that produces myxoxanthophyll but not zeaxanthin owing to the shared requirement of CrtR for synthesis of both carotenoids, however, myxoxanthophyll biosynthesis is specifically halted at the first dedicated step, 1′,2′-hydroxylation of lycopene/γ-carotene, in the absence of the C-1′-hydroxylase CruF (**Figure S3)** (45, 46). Deletion of *cruF* generated a mutant that did not contain any myxoxanthophyll or myxoxanthophyll-specific precursors but otherwise had a normal carotenoid quota; *cruF* deletion in the Δ*crtR* strain resulted in a strain that lacks 3-dehydroxy-myxoxanthophyll as well as zeaxanthin and myxoxanthophyll, accumulating only β-carotene and echinenone in significant amounts (**Figure S2**). The only other confirmed enzyme in myxoxanthophyll biosynthesis in cyanobacteria is the 2′-O-glycosyltransferase CruG, which adds a sugar moiety to the carotenoid backbone (**Figure S3;** 45). Deletion of the *Synechocystis cruG* homologue from the WT and Δ*crtR* strains resulted in accumulation of myxol or 3-dehydroxy-myxol, respectively (**Figure S2**). Finally, we constructed a Δ*crtO* mutant lacking the FAD-dependent β-ionone ring ketolase, which produces myxoxanthophyll and zeaxanthin but is unable to synthesise the keto-carotenoids echinenone and 3′-hydroxy-echinenone (43).

The *in vitro* interaction of ChlG and HliD requires zeaxanthin

Parallel immunoprecipitations of FLAG-ChlG (F.ChlG) from the FG/ΔG strain and the carotenoid mutants were performed to investigate the effect of xanthophyll deficiency on the ChlG-HliD interaction *in vitro* (**Figure 2**). Retrieval of F.ChlG from each strain was confirmed by SDS-PAGE (**Figure 2A**) and immunoblotting with FLAG and ChlG specific primary antibodies (**Figure 2B**). F.ChlG from the FG/ΔG strain co-eluted with both HliD and Ycf39 as observed previously (21, 27); note that F.ChlG from strains lacking *crtR* migrated slightly further than expected on SDS-PAGE gels, which is discussed below.

Only a residual immunoblot signal for HliD was observed in the FG/ΔG/Δ*crtR* and FG/ΔG/Δ*crtR*/Δ*cruF* eluates, accompanied by the loss of signal for Ycf39; the level of HliD was comparable in thylakoids isolated from each of the strains (**Figure 2C**), ruling out the possibility of any pleiotropic effect on the production of HliD associated with deletion of *crtR*. Consistent with the absence of HliD, direct measurement of the absorbance spectra of the eluates from the FG/ΔG/Δ*crtR* and FG/ΔG/Δ*crtR*/Δ*cruF* strains revealed a drastic reduction in pigmentation compared to the visibly orange eluate from the

FG/ΔG strain (**Figure 2D**). Qualitative analysis of the pigments in the eluates by RP-HPLC confirmed Chl, β-carotene myxoxanthophyll and zeaxanthin were present in the complex isolated from the FG/ΔG strain (**Figure 2E**). Small amounts of dehydroxy-myxoxanthophyll, Chl and β-carotene were present in the FG/ΔG/Δ*crtR* elution; the Chl and β-carotene likely originate from trimeric PSI which contaminates FLAG-tag pulldowns (21).

In contrast to those from strains lacking *crtR*, FLAG-immunoprecipitation eluates from the FG/ΔG/Δ*cruF* mutant were visibly orange and spectrally similar to those from the FG/ΔG parent strain (**Figure 2D**). Immunoblot analysis of the FG/ΔG/Δ*cruF* eluate gave clear signals for both HliD and Ycf39 and zeaxanthin was identified by RP-HPLC analysis of the extracted pigments (**Figure 2B, E**). Removing the sugar group from myxoxanthophyll (producing myxol) or dehydroxy-myxoxanthophyll (producing dehydroxy-myxol) by deletion of *cruG* from the FG/ΔG and FG/ΔG/Δ*crtR* backgrounds, respectively, did not alter the results compared to those of the respective parent strain (**Figure S5**). Finally, deletion of *crtO* did not affect the composition of the F.ChlG complex (**Figure S6**), confirming that keto-carotenoids are not involved in the ChlG-HliD interaction.

Quantitative proteomic analysis by mass-spectrometry was also used to compare the levels of HliD and Ycf39 co-isolated with F.ChlG from the different carotenoid mutants (**Figure 2F**). When normalised to the amount of bait protein, the absence of myxoxanthophyll (FG/ΔG/Δ*cruF*) did not significantly change the amount of HliD co-purified with F.ChlG compared to the FG/ΔG control (P = 0.35). However, the absence of zeaxanthin (in the FG/ΔG/Δ*crtR* strain) or both zeaxanthin and myxoxanthophyll (in FG/ΔG/Δ*crtR*/Δ*cruF*) drastically reduced the level of HliD to 2-3% of the control level (**Table S2**). These effects on the HliD:F.ChlG stoichiometry were mirrored by that of Ycf39:F.ChlG, with no significant change after elimination of myxoxanthophyll (P = 0.67) and average decreases to 10-20% of the control level in the zeaxanthin-less strains.

The protein tag does not affect formation of the ChlG complex

As stated above, F.ChlG isolated from strains lacking *crtR* migrated slightly faster on SDS-PAGE gels (**Figure 2A**), suggesting the protein was somehow smaller. Sequencing of the *psbAII* locus in these FG/ΔG/Δ*crtR* strains confirmed the loss of one of the 3×FLAG-epitopes, leaving a 2×FLAG-tag in frame with the *chlG* gene (**Figure S7**). Using a freshly isolated FG/ΔG/Δ*crtR* mutant confirmed to have the 3×FLAG-tag and performing parallel co-immunoprecipitations alongside a strain with a 2×FLAG-tagged enzyme showed that the length of the tag did not affect the protein or pigment profiles of the eluates (**Figure S8**).

The 3xFLAG-tag is relatively long (24 amino acids) and highly positively charged. To confirm that this extra amino-acid sequence does not generate artefacts regarding the interaction with xanthophylls, the experiments were repeated with an N-terminally 10xHis-tagged ChlG (H.ChlG; **Figure S4** and **S9**). Purification of the His-tagged enzyme by immobilised nickel-affinity chromatography resulted in a visibly pigmented eluate with very similar absorbance properties to the FLAG-immunoprecipitation complex (**Figure S10C**). Analysis of the eluate by SDS-PAGE and immunoblotting showed a prominent band corresponding to H.ChlG (**Figure S10A-B**); immunoblots also confirmed the presence of HliD (**Figure S10B**), and zeaxanthin and myxoxanthophyll were identified by RP-HPLC (**Figure S10D**). Consistent with the results with the FLAG-tagged enzyme (**Figure 2**), HliD does not co-elute with H.ChlG in the absence of zeaxanthin and myxoxanthophyll (**Figure S10A-B**) and the eluate contained very low levels of pigments (**Figure S10C-D**).

Association of xanthophylls with ChlG is dependent on HliD

Previous studies have shown that *Synechocystis* Δ*hliD* mutants do not display a growth phenotype or altered accumulation of photosystems under standard low-stress laboratory growth conditions (47-49). However, deletion of *hliD* did decrease the level of ChlG, resulting in a concomitant six-fold increase in the level of its substrate Chlide *a* (21). We generated an independent *hliD* deletion in the FG/ΔG background (**Figures S2** and **S4**) in order to determine the inherent pigment binding properties of isolated F.ChlG in the absence of HliD. In agreement with previous reports, there was a marked reduction in the level of F.ChlG isolated from FG/ΔG/Δ*hliD* using the same amount of starting material (solubilised thyloakoid membranes), although it was possible to isolate Coomassie-stainable quantities of the protein (**Figure 3A**). As expected, Ycf39 was not detectable by immunoblot (**Figure 3B**) and the eluate lacked Chl and carotenoids, evident from both the absorbance spectra (**Figure 3C**) and RP-HPLC analysis of extracted pigments (**Figure 3D**), confirming that ChlG alone does not bind carotenoids. Consistent with the result obtained with the FLAG-tagged enzyme, isolation of H.ChlG from a Δ*hliD* background also resulted in a decreased level of ChlG (**Figure S10A-B**) and an immobilised nickel-affinity chromatography eluate that lacked pigments (**Figure S10C-D**).

Restoration of the ChlG-xanthophyll-HliD interaction in isolated membranes

The results presented above indicate that xanthophylls are required to maintain the interaction between ChlG and HliD, and that ChlG does not co-purify with carotenoids in the absence of HliD. To determine whether the interaction could be restored in isolated membranes, solubilised membranes

from the FG/ΔG/Δ*hliD* strain, which synthesizes the normal complement of carotenoids but lacks HliD, were incubated with those from the FG/ΔG/Δ*crtR*/Δ*cruF* strain, which lacks zeaxanthin and myxoxanthophyll but produces HliD (schematically illustrated in **Figure 4A**). F.ChlG was subsequently isolated from the individual or mixed membrane samples by immunoprecipitation (**Figure 4B**). Unlike eluates from either individual sample, immunoblotting detected both HliD and Ycf39 in the elution from the mixed membranes (**Figure 4C**). Although considerably less pigmented than that from the FG/ΔG strain, the eluate from the mixed sample was visibly coloured and the absorbance spectra revealed a small but clear increase in pigmentation compared to the eluates from the two mutant strains (**Figure 4D**). Zeaxanthin and myxoxanthophyll were both present in the complex isolated from the combined membranes (**Figure 4E**), confirming that the ChlG-HliD interaction can reform upon provision of xanthophylls. Re-formation of the ChlG-HliD complex was also achieved in an analogous experiment with membranes from the equivalent H.ChlG strains (**Figure S11**).

ChlG-HliD complexes in thylakoid membranes are affected by xanthophyll deficiency

Isolation of FLAG- or His-tagged ChlG complexes requires washing steps that might disrupt interactions with weakly-binding proteins. To further ascertain the effects of the loss of xanthophylls on the ChlG-HliD complex we used an alternative approach, separating solubilised thylakoid membrane proteins by two-dimensional BN/SDS-PAGE followed by immunoblotting (**Figure 5**). Most of the detectable ChlG in WT membranes appears to co-migrate with HliD in a ~100 KDa complex; this complex likely forms the major fraction of our co-immunoprecipitated F.ChlG and it is likely to be composed of ChlG associated with several copies of HliD (21). A larger ChlG-HliD complex is also detected; we refer to the smaller ChlG-HliD assembly as complex 1 and the larger one as complex 2, as indicated above the figure. Small amounts of free ChlG and HliD, and the Ycf39-HliD complex (28), which migrates slightly faster than the ChlG-HliD complex 1, are also clearly observed.

Repeating the analysis with membranes of the Δ*crtR*/Δ*cruF* double mutant lacking both zeaxanthin and myxoxanthophyll, the ratio between the ChlG-HliD complex 1 and unattached ChlG differed from the WT sample, with much less ChlG present in the complex with HliD and more in a free form. Along with the clear reduction in ChlG-HliD complex 1, the larger complex 2 is almost completely absent in the Δ*crtR*/Δ*cruF* mutant. In contrast, the Ycf39-HliD interaction is unaffected by removal of xanthophylls. This 2D-BN/SDS-PAGE analysis supports the proposed requirement for xanthophylls for the stability of the ChlG-HliD complexes in the thylakoid membranes of *Synechocystis*.

Xanthophyll mediated association of ChlG and HliD promotes ChlG function

As discussed above, deletion of *hliD* results in a decreased cellular level of ChlG and accumulation of its substrate, Chlide (21). To determine the effect of the absence of xanthophylls on Chl biosynthesis the levels of Chl and its biosynthetic intermediates (see **Figure S12** for an overview of the Chl biosynthesis pathway) were compared in WT, Δ*crtR*, Δ*cruF* and Δ*crtR*/Δ*cruF* cells (**Figure 6**). Under standard growth conditions the whole cell absorbance spectra were similar for all four strains except for the region where carotenoids absorb (450-500 nm; **Figure 6A**). The Chl level of the Δ*cruF* (4.8±0.3 μg Chl per ml of 1 OD_{750} unit cells) and Δ*crtR*/Δ*cruF* (5.2±0.1 μg ml^{-1}) strains were not significantly different to that of the WT (5.1±0.2 μg ml^{-1}), but the Δ*crtR* mutant did display a small but significant (P = 0.04) decrease in Chl (4.6±0.2 μg ml^{-1}) (**Figure 6B**).

Interestingly, the level of the ChlG substrate monovinyl (MV)-Chlide was 6-7 times higher in the Δ*crtR* and Δ*crtR*/Δ*cruF* mutants compared to the WT (set as 100%) (**Figure 6C**), indicating that ChlG activity is affected by the loss of zeaxanthin. Similarly, divinyl (DV)-Chlide, the substrate of the preceding enzyme in the pathway, 8-vinyl reductase (8VR), also accumulated ~4-fold in both strains compared to the WT, suggesting the 8VR reaction is also affected, either directly or by the build-up of MV-Chlide. In contrast, the Δ*cruF* strain contained both Chlide species at levels comparable to the WT. The only other statistically significant differences in precursor levels were the decrease in magnesium-protoporphyrin IX in the Δ*crtR* mutant and the increase in magnesium protoporphyrin monomethyl ester in Δ*cruF*. The reason(s) for these small variations in earlier pathway intermediates are likely due to pleiotropic effects resulting from the loss of xanthophylls in these strains.

Discussion

We have shown that zeaxanthin stabilises the ChlG-HliD interaction in *Synechocystis* membranes. The alternating single-double carbon-carbon bonds in the polyene chain of carotenoids makes them much more rigid than other hydrophobic molecules, such as comparatively flexible lipids, and a scaffolding role for carotenoids in LHC proteins in plants has been proposed previously (reviewed by 13). Although HliD and ChlG still associate to a minor extent in the absence of both zeaxanthin and myxoxanthophyll, this complex appears to be considerably less stable than in WT cells since the HliD protein is almost completely absent in F.ChlG immunoprecipitation eluates from a Δ*crtR* mutant. Therefore, neither β-carotene, echinenone nor dehydroxy-myxoxanthophyll (myxoxanthophyll with an unhydroxylated β-ring which accumulates in the Δ*crtR* mutant (35, 44)) can substitute for zeaxanthin/myxoxanthophyll in stabilising the ChlG-HliD interaction. These results suggest that the hydroxyl groups on the β ring(s)

of zeaxanthin and myxoxanthophyll, which allow xanthophylls to be held perpendicular to the membrane through strong hydrogen bonds, enhancing their structural function (13), are essential for their interaction with ChlG and HliD. Another Hlip (HliA/B) pigment-protein complex has also been reported to contain zeaxanthin and myxoxanthophyll (50), while zeaxanthin binds to the conserved C-terminal transmembrane Chl *a*/*b* binding (CAB) domains of dimeric ferrochelatase (25); thus, xanthophylls may play similar roles in other Hlip-/CAB-domain protein assemblies in *Synechocystis*.

The ChlG-HliD interaction was maintained in a Δ*cruF* mutant that produces zeaxanthin but not myxoxanthophyll, indicating that zeaxanthin alone can mediate association of the two proteins. However, reconstitution of the ChlG-HliD interaction in isolated membranes showed both myxoxanthophyll and zeaxanthin were incorporated into the re-formed complex; thus, promiscuity versus specificity of zeaxanthin and myxoxanthophyll binding sites in the ChlG-HliD complex requires further study. Insight into any specific role of myxoxanthophyll requires a strain that produces myxoxanthophyll in the absence of zeaxanthin, but this is not possible by deletion of native genes because of the shared requirement of CrtR for biosynthesis of both carotenoids. We attempted to generate such a strain using CrtR from the filamentous cyanobacteria *Nostoc* sp. PCC 7120 (alr4009), which produces keto-myxoxanthophyll species but does not synthesise zeaxanthin (51-53). However, our preliminary results indicate that neither myxoxanthophyll nor zeaxanthin biosynthesis was restored when alr4009 was expressed in place of the native *crtR* or at the *psbAII* locus in the Δ*crtR* mutant (data not shown).

Isolation of native ChlG complexes from other chlorophototrophic organisms has not yet been reported but given the high-level of sequence conservation of cyanobacterial ChlG enzymes (e.g., 84% identity in *Synechocystis* and *Synechococcus* sp. PCC 7002) we predict that ChlG-xanthophyll-HliD complexes will be conserved in cyanobacteria. In support of this, we previously reported that ChlG from *Synechococcus* sp. PCC 7002, produced in *Synechocystis*, interacts with HliD, zeaxanthin and myxoxanthophyll (27). The myxoxanthophyll species produced in *Synechocystis* is myxol-2' dimethylfucoside, whereas *Synechococcus* sp. PCC 7002 produces myxol-2' fucoside, which lacks two methyl groups on the sugar moiety (45, 54), indicating that the fucose group is not important for the interaction of myxoxanthophyll with the complex, as found with the Δ*cruG* mutant here.

Although we cannot rule out that altered thylakoid membrane carotenoid content in the xanthophyll mutants may affect the detergent-sensitivity of protein complexes, our data still supports a role for xanthophylls in stabilising the interaction of ChlG and HliD. Destabilising this association by removal of xanthophylls or deletion of HliD results in a significant build-up of Chlide and, in the latter case, the accumulation of ChlG is also reduced. However, consistent with previous results, there are no major

phenotypic consequences relating to growth or chlorophyll biosynthesis upon the loss of HliD, at least under our standard, low-stress laboratory growth conditions. It is possible that the ChlG-xanthophylls-HliD complex is particularly important under specific stress-conditions. For example, the xanthophylls could quench singlet oxygen produced during photo-oxidative stress; work is underway to elucidate how xanthophyll-mediated recruitment of HliD affects Chl metabolism in cyanobacteria *in vivo*.

In contrast to cyanobacterial ChlG, the enzymes from *Arabidopsis thaliana* (Arabidopsis) and the green alga *Chlamydomonas reinhardtii* do not associate with HliD or xanthophylls when heterologously produced in *Synechocystis* (27). These phototrophs lack Hlips, and decreased sequence identity between plant and cyanobacterial ChlG (e.g., 63% for Arabidopsis and *Synechocystis*) may explain why the eukaryotic enzymes do not interact with HliD. Plants do, however, contain single helix LHC-like proteins that are homologous to Hlips called One-Helix Proteins (OHPs) (**Figure S13**) (55). Like HliD and HliC, which are predicted to form heterodimers in cyanobacteria (22, 28), Arabidopsis OHP1 and OHP2 have been shown to dimerise *in vivo* (56). Furthermore, OHPs bind the plant homolog of Ycf39 (HCF244) and are suggested to function in pigment delivery to newly synthesized PSII subunits (56-58), as proposed for the cyanobacterial Ycf39-Hlip complex (28, 59). It is currently unclear whether Ycf39-Hlip-dependent synthesis of PSII subunits relies on the additional interaction of Hlips with ChlG. If so, then OHPs (and HCF244) may associate with ChlG in plants as well, although evidence of such a complex is yet to be reported. Plants also synthesise LIL3 (55), a two transmembrane helix protein with a proposed role in Chl biosynthesis; LIL3 interacts with the Chl biosynthesis enzymes protochlorophyllide oxidoreductase (POR) and geranylgeranyl diphosphate reductase (ChlP), although whether it forms a complex with ChlG is not clear and may be species-specific (60-62). Further work is required to clarify the interactions between these LHC-like proteins and Chl biosynthesis enzymes in plants, but it is feasible that zeaxanthin and/or other abundant plant xanthophylls, such as lutein, may play stabilization roles in such complexes.

Competing Interests: The authors declare that there are no competing interests associated with the manuscript.

Author contributions: M.S.P., D.P.C., C.N.H., R.S. and A.H. conceived the study and designed the experiments. M.P.J., C.N.H., R.S. and A.H. supervised the project. M.S.P., M.P., P.J.J., J.P., E.C.M., M.J.D., R.S. and A.H. performed the experiments and/or analysed the data. M.S.P., R.S. and A.H. wrote the manuscript.

Funding: M.S.P. was supported by a University of Sheffield Faculty of Science PhD Studentship. M.P., J.P. and R.S. were supported by grant 19-29225X from the Czech Science Foundation. M.J.D. acknowledges award BB/M012166/1 from the Biotechnology and Biological Sciences Research Council (BBSRC) UK. M.P.J. acknowledges award RPG-2019-045 from the Leverhulme Trust. C.N.H. acknowledges funding from the European Research Council (Synergy Award 854126) and the BBSRC UK (award BB/M000265/1). A.H. acknowledges support from a Royal Society University Research Fellowship (award number URF\R1\191548).

Abbreviations

β-DDM ,n-dodecyl-β-maltoside; BN-PAGE, blue native polyacrylamide gel electrophoresis; Chl(s), chlorophyll(s); Chlide, chlorophyllide; ChlG, chlorophyll synthase; F.ChlG, FLAG-chlorophyll synthase; H.ChlG, His-chlorophyll synthase; Hlips, high-light-inducible proteins; HliC, high-light-inducible protein C; HliD, high light inducible protein D; LHCs, light-harvesting complexes; RP-HPLC, reverse phase high-performance liquid chromatography; SDS-PAGE, sodium dodecyl sulfate polyacrylamide gel electrophoresis; PSI, photosystem I, PSII, photosystem II; WT, wild-type.

References

(1) Frank, H.A. and Cogdell, R.J. (1996) Carotenoids in Photosynthesis. *Photochem. Photobiol.* **63**, 257-264 https://doi.org/10.1111/j.1751-1097.1996.tb03022.x

(2) Hashimoto, H., Uragami, C. and Cogdell, R.J. (2016) Carotenoids and Photosynthesis. In: Stange C. (eds) Carotenoids in Nature. Subcellular Biochemistry, vol 79. Springer, Cham. https://doi.org/10.1007/978-3-319-39126-7_4

(3) Jordan, P., Fromme, P., Witt, H.T., Klukas, O., Saenger, W. and Krausz, N. (2001) Three-dimensional structure of cyanobacterial photosystem I at 2.5 Å resolution. *Nature* **411**, 909–917 https://doi.org/10.1038/35082000

(4) Sozer, O., Komenda, J., Ughy, B., Domonkos, I., Laczkó-Dobos, H., Malec, P. et al (2010) Involvement of carotenoids in the synthesis and assembly of protein subunits of photosynthetic reaction centers of *Synechocystis* sp. PCC 6803. *Plant Cell Physiol*. **51**, 823-835 https://doi.org/10.1093/pcp/pcq031

(5) Tóth, T.N., Chukhutsina, V., Domonkos, I., Knoppová, J., Komenda, J., Kis, M. et al (2015) Carotenoids are essential for the assembly of cyanobacterial photosynthetic complexes. *Biochim. Biophys. Acta*. **1847**, 1153-1165 https://doi.org/10.1016/j.bbabio.2015.05.020

(6) Malavath, T., Caspy, I., Netzer-El, S.Y., Klaiman, D. and Nelson, N. (2018) Structure and function of wild-type and subunit-depleted photosystem I in *Synechocystis*. *Biochim. Biophys. Acta. Bioenerg.* **1859**, 645-654 https://doi.org/10.1016/j.bbabio.2018.02.002

(7) Masamoto, K., Misawa, N., Kaneko, T., Kikuro, T. and Toh, H. (1998) Beta-carotene hydroxylase gene from the cyanobacterium *Synechocystis* sp. PCC6803. *Plant Cell Physiol*. **39**, 560-564 https://doi.org/10.1093/oxfordjournals.pcp.a029405

(8) Umena, Y., Kawakami, K., Shen, J.R. and Kamiya, N. (2011) Crystal structure of oxygen-evolving photosystem II at a resolution of 1.9Å. *Nature* **473**, 55–60 https://doi.org/10.1038/nature09913

(9) Kurisu, G., Zhang, H., Smith, J.L. and Cramer, W.A. (2003) Structure of the cytochrome b_6f complex of oxygenic photosynthesis: tuning the cavity. *Science* **302**, 1009-1014 https://doi.org/10.1126/science.1090165

(10) Malone, L.A., Qian, P., Mayneord, G.E., Hitchcock, A., Farmer, D.A., Thompson, R.F. et al (2019) Cryo-EM structure of the Spinach cytochrome b_6f complex at 3.6 Å resolution. *Nature* **575**, 535-539 https://doi.org/10.1038/s41586-019-1746-6

(11) Schuller, J.M., Birrell, J.A., Tanaka, H., Konuma, T., Wulfhorst, H., Cox, N. et al (2019) Structural adaptations of photosynthetic complex I enable ferredoxin-dependent electron transfer. *Science* **363**, 257-260 https://doi.org/10.1126/science.aau3613.

(12) Havaux, M., Dall'Osto, L. and Bassi, R. (2007) Zeaxanthin has enhanced antioxidant capacity with respect to all other xanthophylls in Arabidopsis leaves and functions independent of binding to PSII antennae. *Plant Physiol*. **145**, 1506–1520 https://doi.org/10.1104/pp.107.108480

(13) Ruban, A.V. and Johnson, M.P. (2010) Xanthophylls as modulators of membrane protein function. *Arch. Biochem. Biophys*. **504**, 78-85 https://doi.org/10.1016/j.abb.2010.06.034

(14) Ruban, A.V. (2016) Nonphotochemical fluorescence quenching: mechanism and effectiveness in protecting plants from photodamage. *Plant Physiol*. **170**, 1903–1916 https://doi.org/10.1104/pp.15.01935

(15) Gruszecki, W.I. and Strzałka, K. (2005) Carotenoids as modulators of lipid membrane physical properties. *Biochim. Biophys. Acta*. **1740**, 108-115 https://doi.org/10.1016/j.bbadis.2004.11.015

(16) Domonkos, I., Kis, M., Gombos, Z. and Ughy, B. (2013) Carotenoids, versatile components of oxygenic photosynthesis. *Prog. Lipid Res*. **52**, 539-561 https://doi.org/10.1016/j.plipres.2013.07.001

(17) Zhu, Y., Graham, J.E., Ludwig, M., Xiong, W., Alvey, R.M., Shen, G. et al (2010) Roles of xanthophyll carotenoids in protection against photoinhibition and oxidative stress in the cyanobacterium *Synechococcus* sp. strain PCC 7002. *Arch. Biochem. Biophys*. **504**, 86-99 https://doi.org/10.1016/j.abb.2010.07.007

(18) Kusama, Y., Inoue, S., Jimbo, H., Takaichi, S., Sonoike, K., Hihara, Y. et al (2015) Zeaxanthin and echinenone protect the repair of photosystem II from inhibition by singlet oxygen in *Synechocystis* sp. PCC 6803. *Plant Cell Phys.* **56**, 906–916 https://doi.org/10.1093/pcp/pcv018

(19) Vajravel, S., Kis, M., Kłodawska, K., Laczko-Dobos, H., Malec, P., Kovács, L. et al (2017) Zeaxanthin and echinenone modify the structure of photosystem I trimer in *Synechocystis* sp. PCC 6803. *Biochim. Biophys. Acta. Bioenerg*. **1858**, 510-518 https://doi.org/10.1016/j.bbabio.2017.05.001

(20) Kerfeld, C.A., Melnicki M.R., Sutter, M. and Dominguez-Martin, M.A. (2017) Structure, function and evolution of the cyanobacterial orange carotenoid protein and its homologs. *New Phytol*. **215**, 937-951 https://doi.org/10.1111/nph.14670

(21) Chidgey, J.W., Linhartová, M., Komenda, J., Jackson, P.J., Dickman, M.J., Canniffe, D.P. et al (2014) A cyanobacterial chlorophyll synthase-HliD complex associates with the Ycf39 protein and the YidC/Alb3 insertase. *Plant Cell* **26**, 1267–1279 https://doi.org/10.1105/tpc.114.124495

(22) Niedzwiedzki, D.M., Tronina, T., Liu, H., Staleva, H., Komenda, J., Sobotka, R. et al (2016) Carotenoid-induced non-photochemical quenching in the cyanobacterial chlorophyll synthase-HliC/D complex. *Biochim. Biophys. Acta*. **1857**, 1430-1439 https://doi.org/10.1016/j.bbabio.2016.04.280

(23) Dolganov, N.A., Bhaya, D. and Grossman A.R. (1995) Cyanobacterial protein with similarity to the chlorophyll *a*/*b* binding proteins of higher plants: evolution and regulation. *Proc. Natl. Acad. Sci*. U.S.A. **92**, 636-640 https://doi.org/10.1073/pnas.92.2.636

(24) Komenda, J. and Sobotka, R. (2016) Cyanobacterial high-light-inducible proteins - Protectors of chlorophyll-protein synthesis and assembly. *Biochim. Biophys. Acta.* **1857**, 288–295 https://doi.org/10.1016/j.bbabio.2015.08.011

(25) Pazderník, M., Mareš, J., Pilný, J. and Sobotka, R. (2019) The antenna-like domain of the cyanobacterial ferrochelatase can bind chlorophyll and carotenoids in an energy-dissipative configuration. *J. Biol. Chem*. **294**, 11131-11143 https://doi.org/10.1074/jbc.RA119.008434

537 (26) Kiefer, D. and Kuhn, A. (2018) YidC-mediated membrane insertion. *FEMS Microbiol. Lett*. **365**, 12
538 https://doi.org/10.1093/femsle/fny106

539 (27) Proctor, M.S., Chidgey, J.W., Shukla, M.K., Jackson, P.J., Sobotka, R., Hunter, C.N. et al (2018) Plant
540 and algal chlorophyll synthases function in *Synechocystis* and interact with the YidC/Alb3 membrane
541 insertase. *FEBS Lett*. **18**, 3062-3073 https://doi.org/10.1002/1873-3468.13222

542 (28) Knoppová, J., Sobotka, R., Tichý, M., Yu, J, Konik P, Halada P et al (2014) Discovery of a Chlorophyll
543 Binding Protein Complex Involved in the Early Steps of Photosystem II Assembly in *Synechocystis*. *Plant*
544 *Cell* **26**, 1200-1212 https://doi.org/10.1105/tpc.114.123919

545 (29) Shukla, M.K., Llansola-Portoles, M.J., Tichý, M., Pascal, A.A., Robert, B. and Sobotka, R. (2018)
546 Binding of pigments to the cyanobacterial high-light-inducible protein HliC. *Photosynth. Res*. **137**, 29-
547 39 https://doi.org/10.1007/s11120-017-0475-7

548 (30) Staleva, H., Komenda, J., Shukla, M.K., Šlouf, V., Kaňa, R., Polívka, T. et al (2015) Mechanism of
549 photoprotection in the cyanobacterial ancestor of plant antenna proteins. *Nat. Chem. Biol*. **11**, 287–
550 291 https://doi.org/10.1038/nchembio.1755

551 (31) Llansola-Portoles, M.J., Sobotka, R., Kish, E., Shukla, M.K., Pascal, A.A., Polivka, T. et al (2017)
552 Twisting a β-Carotene, an Adaptive Trick from Nature for Dissipating Energy during Photoprotection.
553 *J. Biol. Chem.* **292**, 1396-1403 https://doi.org/10.1074/jbc.M116.753723

554 (32) Rippka, R., Derueles, J., Waterbury, J.B., Herdman, M. and Stainer, R.Y. (1979) Generic
555 Assignments, Strain Histories and Properties of Pure Cultures of Cyanobacteria. *J. Gen. Microbiol.* **111**,
556 1-61 https://doi.org/10.1099/00221287-111-1-1

557 (33) Tichý, M., Bečková, M., Kopečná, J., Noda, J., Sobotka, R. and Komenda, J. (2016) Strain of
558 *Synechocystis* PCC 6803 with Aberrant Assembly of Photosystem II Contains Tandem Duplication of a
559 Large Chromosomal Region. *Front. Plant Sci*. **7**, 648 https://doi.org/10.3389/fpls.2016.00648

560 (34) Xu, H., Vavilin, D., Funk, C. and Vermaas, W. (2004) Multiple deletions of small Cab-like proteins
561 in the cyanobacterium *Synechocystis* sp. PCC 6803: consequences for pigment biosynthesis and
562 accumulation. *J. Biol. Chem*. **279**, 27971-27979 https://doi.org/10.1074/jbc.M403307200

563 (35) Lagarde, D. and Vermaas, W. (1999) The zeaxanthin biosynthesis enzyme β-carotene hydroxylase
564 is involved in myxoxanthophyll synthesis in *Synechocystis* sp. PCC 6803. *FEBS Lett*. **454**, 247-251
565 https://doi.org/10.1016/s0014-5793(99)00817-0

(36) Hitchcock, A., Jackson, P.J., Chidgey, J.W., Dickman, M.J., Hunter, C.N. and Canniffe, D.P. (2016) Biosynthesis of Chlorophyll *a* in a Purple Bacterial Phototroph and Assembly into a Plant Chlorophyll-Protein Complex. *ACS Synth. Biol*. **5**, 948-954 https://doi.org/10.1021/acssynbio.6b00069

(37) MacGregor-Chatwin, C., Jackson, P.J., Sener, M., Chidgey, J.W., Hitchcock, A., Qian, P. et al (2019) Membrane organisation of photosystem I complexes in the most abundant phototroph on Earth. *Nat. Plants* **5**, 879-889 https://doi.org/10.1038/s41477-019-0475-z

(38) Cox, J. and Mann, M. (2008) MaxQuant enables high peptide identification rates, individualized p.p.b.-range mass accuracies and proteome-wide protein quantification. *Nat. Biotechnol*. **26**, 1367–1372 https://doi.org/10.1038/nbt.1511

(39) Porra, R.J., Thompson, W.A. and Kriedemann, P.E. (1989) Determination of accurate extinction coefficients and simultaneous equations for assaying chlorophylls a and b extracted with four different solvents: verification of the concentration of chlorophyll standards by atomic absorption spectroscopy. *Biochim. Biophys. Acta*. **975**, 384-394 https://doi.org/10.1016/S0005-2728(89)80347-0

(40) Pilný, J., Kopečná, J., Noda, J. and Sobotka, R. (2015) Detection and Quantification of Heme and Chlorophyll Precursors Using a High Performance Liquid Chromatography (HPLC) System Equipped with Two Fluorescence Detectors. *Bio-Protocol* **5**, e1390 https://doi.org/10.21769/BioProtoc.1390

(41) Maresca, J.A., Graham, J.E. and Bryant, D.A. (2008) The biochemical basis for structural diversity in the carotenoids of chlorophototrophic bacteria. *Photosynth. Res*. **97**, 121-140 https://doi.org/10.1007/s11120-008-9312-3

(42) Graham, J.E. and Bryant, D.A. (2008) The Biosynthetic pathway for synechoxanthin, an aromatic carotenoid synthesized by the euryhaline, unicellular cyanobacterium *Synechococcus* sp. strain PCC 7002. *J. Bacteriol*. **190**, 7966-7974 https://doi.org/10.1128/JB.00985-08

(43) Fernández-González, B., Sandmann, G. and Viogue, A. (1997) A new type of asymmetrically acting beta-carotene ketolase is required for the synthesis of echinenone in the cyanobacterium *Synechocystis* sp. PCC 6803. *J. Biol. Chem*. **272**, 9728-9733 https://doi.org/10.1074/jbc.272.15.9728

(44) Schäfer, L., Vioque, A. and Sandmann, G. (2005) Functional in situ evaluation of photosynthesis-protecting carotenoids in mutants of the cyanobacterium *Synechocystis* PCC6803. *J. Photochem. Photobiol. B*. **78**, 195-201 https://doi.org/10.1016/j.jphotobiol.2004.11.007

(45) Graham, J.E. and Bryant, D.A. (2009) The biosynthetic pathway for myxol-2' fucoside (myxoxanthophyll) in the cyanobacterium *Synechococcus* sp. strain PCC 7002. *J. Bacteriol*. **191**, 3292-3300 https://doi.org/10.1128/JB.00050-09

(46) Vajravel, S., Kovács, L., Kis, M., Rehman, A.U., Vass, I., Gombos, Z. et al (2016) β-carotene influences the phycobilisome antenna of cyanobacterium *Synechocystis* sp. PCC 6803. *Photosynth. Res*. **130**, 403-415 https://doi.org/10.1007/s11120-016-0273-7

(47) Funk, C. and Vermaas, W. (1999) A cyanobacterial gene family coding for single-helix proteins resembling part of the light-harvesting proteins from higher plants. *Biochemistry* **38**, 9397-9404 https://doi.org/ 10.1021/bi990545+

(48) He, Q., Dolganov, N., Bjorkman, O. and Grossman, A.R. (2001) The high light-inducible polypeptides in Synechocystis PCC6803. Expression and function in high light. *J. Biol. Chem*. **276**, 306-314 https://doi.org/ 10.1074/jbc.M008686200

(49) Wang, Q., Jantaro, S., Lu, B., Majeed, W., Baily, M. and He, Q. (2008) The High Light-Inducible Polypeptides Stabilize Trimeric Photosystem I Complex under High Light Conditions in *Synechocystis* PCC 6803. *Plant Physiol*. **147**, 1239-1250 https://doi.org/10.1104/pp.108.121087

(50) Daddy, S., Zhan J., Jantaro, S., He, C., He, Q. and Wang, Q. (2015) A Novel High Light-Inducible Carotenoid-Binding Protein Complex in the Thylakoid Membranes of *Synechocystis* PCC 6803. *Sci. Rep*. **5**, 9480 https://doi.org/10.1038/srep09480

(51) Takaichi, S., Mochimaru, M., Maoka, T. and Masamoto, K. (2005) Myxol and 4-ketomyxol 2'-fucosides, not rhamnosides, from Anabaena sp. PCC 7120 and Nostoc punctiforme PCC 73102, and proposal for the biosynthetic pathway of carotenoids. *Plant Cell Physiol*. **46**, 497-504 https://doi.org/10.1093/pcp/pci049

(52) Makino, T., Harada, H., Ikenaga, H., Matsuda, S., Takaichi, S., Shindo, K. et al (2008) Characterization of cyanobacterial carotenoid ketolase CrtW and hydroxylase CrtR by complementation analysis in *Escherichia coli*. *Plant Cell Physiol*. **49**, 1867-1878 https://doi.org/ 10.1093/pcp/pcn169

(53) Mochimaru, M., Masukawa, H., Maoka, T., Mohamed, H.E., Vermaas, W.F. and Takaichi, S. (2008) Substrate specificities and availability of fucosyltransferase and beta-carotene hydroxylase for myxol 2'-fucoside synthesis in *Anabaena* sp. strain PCC 7120 compared with *Synechocystis* sp. strain PCC 6803. *J. Bacteriol.* **190**, 6726-6733 https://doi.org/10.1128/JB.01881-07

(54) Takaichi, S., Maoka, T. and Masamoto, K. (2001) Myxoxanthophyll in *Synechocystis* sp. PCC 6803 is myxol 2'-dimethyl-fucoside, (3R,2S)-myxol 2'-(2,4-di-O-methyl-α-L-fucoside), not rhamnoside. *Plant Cell Physiol.* **42**, 756-762 https://doi.org/10.1093/pcp/pce098

627 (55) Engelken, J., Brinkmann, H. and Adamska, I. (2010) Taxonomic distribution and origins of the
628 extended LHC (light-harvesting complex) antenna protein superfamily. *BMC Evol. Biol*. **10,** 233
629 https://doi.org/10.1186/1471-2148-10-233

630 (56) Hey, D. and Grimm, B. (2020) ONE-HELIX PROTEIN1 and 2 Forms Heterodimers to Bind Chlorophyll
631 in Photosystem II Biogenesis. *Plant Physiol.* **183**, 179-193 https://doi.org/10.1104/pp.19.01304

632 (57) Hey, D. and Grimm,B. (2018) ONE-HELIX PROTEIN 2 (OHP2) is required for the stability of OHP1
633 and assembly factor HCF244 and is functionally linked to PSII biogenesis. *Plant Physiol.* **177**, 1453-1472
634 https://doi.org/10.1104/pp.18.00540

635 (58) Li, Y., Liu, B., Zhang, J., Kong, F., Zhang, L., Meng, H. et al (2019) OHP1, OHP2, and HCF244 Form a
636 Transient Functional Complex with the Photosystem II Reaction Center. *Plant Physiol*. **179**, 195–208
637 https://doi.org/10.1104/pp.18.01231

638 (59) Knoppová, J. and Komenda, J. (2019) Sequential deletions of photosystem II assembly factors
639 Ycf48, Ycf39 and Pam68 result in progressive loss of autotrophy in the cyanobacterium *Synechocystis*
640 PCC 6803. *Folia Microbiol. (Praha)* **64***,* 683-689 https://doi.org/10.1007/s12223-019-00736-w

641 (60) Tanaka, R., Rothbart, M., Oka, S., Takabayashi, A., Takahashi, K., Shibata, M. et al (2010) LIL3, a
642 light-harvesting-like protein, plays an essential role in chlorophyll and tocopherol biosynthesis. *Proc.*
643 *Natl. Acad. Sci. U. S. A.* **107**, 16721-16725 https://doi.org/10.1073/pnas.1004699107

644 (61) Mork-Jansson, A., Bue, A.K., Gargano, D., Furnes, C., Reisinger, V., Arnold, J. et al (2015) Lil3
645 Assembles with Proteins Regulating Chlorophyll Synthesis in Barley. *PLos ONE* **10**, e0133145
646 https://doi.org/10.1371/journal.pone.0133145

647 (62) Hey, D., Rothbart, M., Herbst, J., Wang, P., Müller, J., Wittmann, D. et al (2017) LIL3, a Light-
648 Harvesting Complex Protein, Links Terpenoid and Tetrapyrrole Biosynthesis in *Arabidopsis thaliana*.
649 *Plant Physiol.* **174**, 1037-1050 https://doi.org/10.1104/pp.17.00505

Tables (1-2) and Figures (1-6)

Table 1. *Synechocystis* strains used in this study. Mutations were generated in the WT, FG/ΔG and HG/ΔG backgrounds, as detailed in the text.

Strain	Properties	Reference/source
Wild-type (WT)	Glucose tolerant WT-P substrain of *Synechocystis* sp. PCC 6803	33
FG/ΔG	N-terminally 3xFLAG-tagged *Synechocystis* sp. PCC 6803 *chlG* inserted in place of *psbAII* and deletion of native *chlG* gene; kanamycin resistant (Kan^R) and zeocin resistance (Zeo^R)	27
HG/ΔG	N-terminally 10xHis-tagged *Synechocystis* sp. PCC 6803 *chlG* inserted in place of *psbAII* and deletion of native *chlG* gene; Kan^R and Zeo^R	This study
Δ*crtR*	Deletion of *crtR* (sll1468); erythromycin resistant (Em^R)	This study
Δ*cruF*	Deletion of *cruF* (sll0814); streptomycin resistant (Sm^R)	This study
Δ*crtO*	Deletion of *crtO* (slr0088); chloramphenicol resistant (Cm^R)	This study
Δ*cruG*	Deletion of *cruG* (sll1004); Sm^R	This study
Δ*crtR*/Δ*cruF*	Deletion of *cruF* in Δ*crtR* background; Em^R and Sm^R	This study
Δ*crtR*/Δ*cruG*	Deletion of *cruG* in Δ*crtR* background; Em^R and Sm^R	This study
Δ*hliD*	Deletion of *hliD* (ssr1789); Em^R	This study

Table 2. Carotenoid deficiencies of *Synechocystis* mutants lacking combinations of *crtR*, *cruF*, *cruG* and *crtO.*

Mutant	Xanthophyll deficiency[a]	Intermediates accumulated
Δ*crtR*	zeaxanthin, cryptoxanthin[b], myxoxanthophyll, 3'-hydroxyechinenone[b]	dehydroxy-myxoxanthophyll
Δ*cruF*	myxoxanthophyll	N/A
Δ*cruG*	myxoxanthothyll	myxol
Δ*crtO*	echinenone, 3'-hydroxyechinenone[b], canthaxanthin[b]	N/A
Δ*crtR* Δ*cruF*	zeaxanthin, cryptoxanthin[b], myxoxanthophyll, 3'-hydroxyechinenone[b]	N/A
Δ*crtR* Δ*cruG*	zeaxanthin, cryptoxanthin[b], myxoxanthophyll, 3'-hydroxyechinenone[b]	dehydroxy-myxol

[a]The xanthophyll deficiency was the same in the WT, FG/ΔG and HG/ΔG backgrounds. [b]These carotenoids were not detected by RP-HPLC in this study; deficiency is assumed based on literature, as detailed in the text and Figure S1.

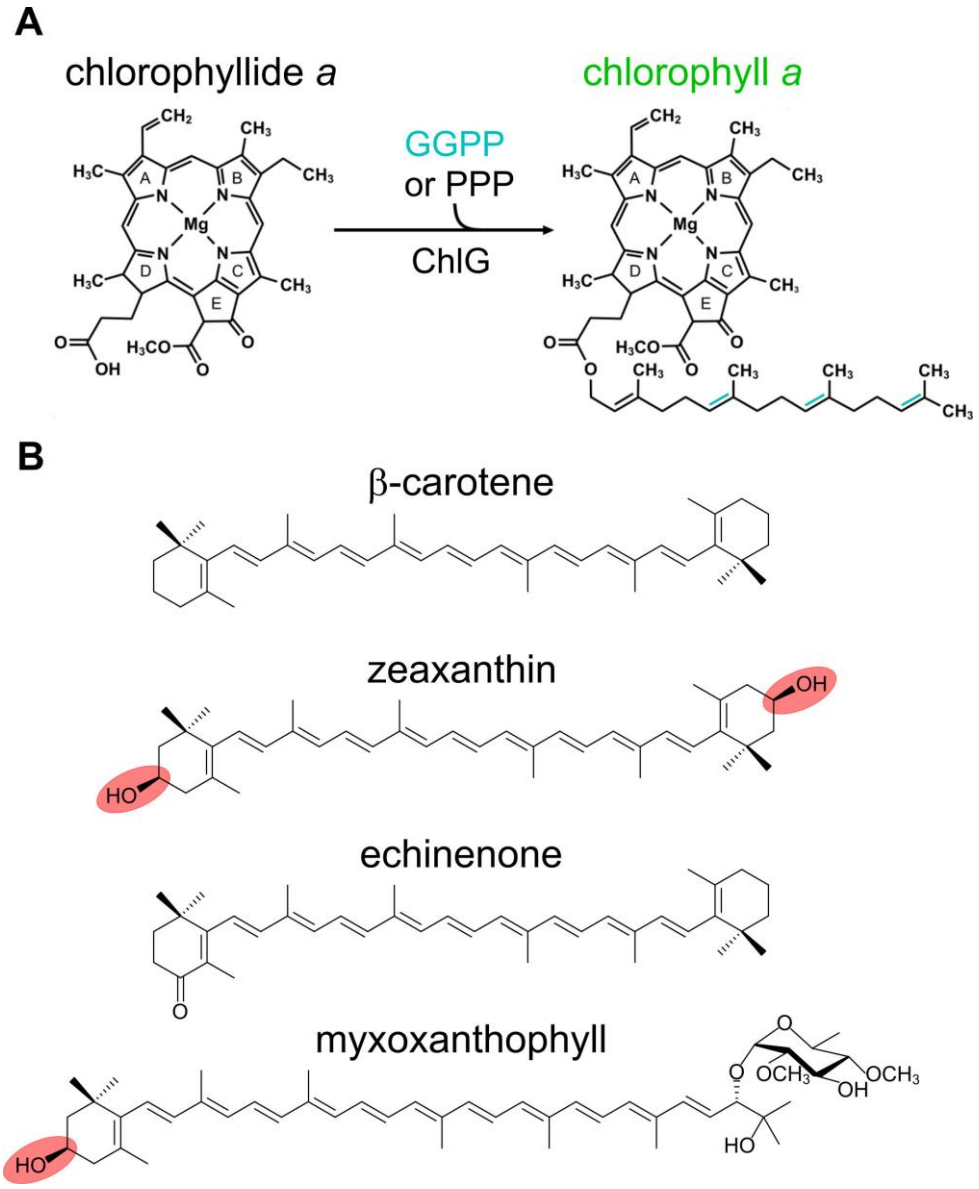

Figure 1. The reaction catalysed by chlorophyll synthase (ChlG) and the molecular structures of the four major carotenoids produced by *Synechocystis*. (A) ChlG esterifies C17 on ring D of chlorophyllide *a* with geranylgeranyl-pyrophosphate (GGPP) or phytyl pyrophosphate (PPP) to produce (GG-)chlorophyll *a*. **(B)** The molecular structures of the four major carotenoids produced by WT *Synechocystis*: β-carotene, zeaxanthin, echinenone and myxoxanthophyll. The hydroxyl groups on the β-rings of zeaxanthin and myxoxanthophyll are highlighted in red.

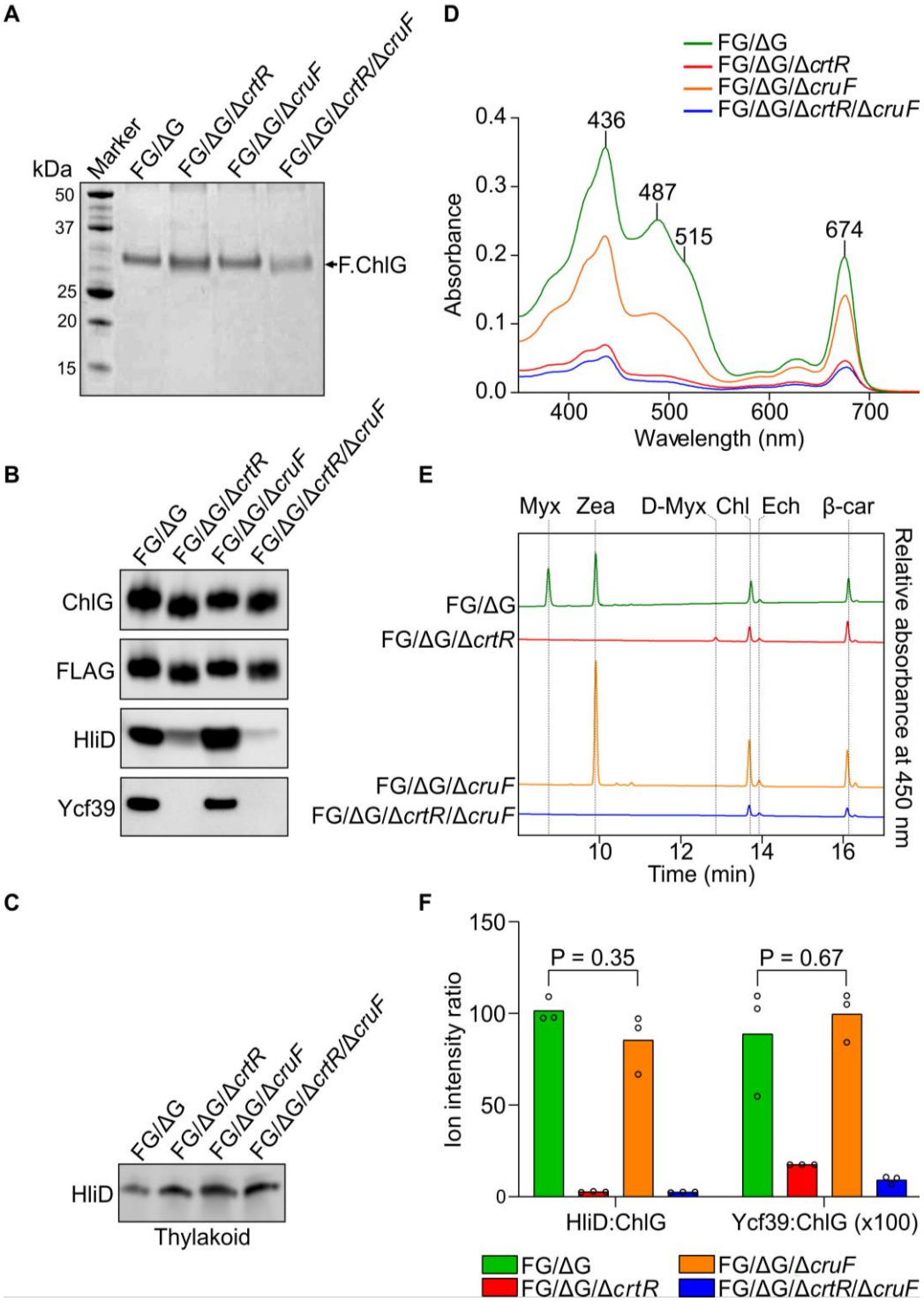

Figure 2. **Analysis of pigment-protein complexes isolated by co-immunoprecipitation of F.ChlG from *Synechocystis* xanthophyll mutants.** (A) Coomassie stained SDS-PAGE analysis of FLAG immunoprecipitation eluates obtained from the FLAG-*chlG* Δ*chlG* (FG/ΔG), FLAG-*chlG* Δ*chlG* Δ*crtR* (FG/ΔG/Δ*crtR*), FLAG-*chlG* Δ*chlG* Δ*cruF* (FG/ΔG/Δ*cruF*) and FLAG-*chlG* Δ*chlG* Δ*crtR* Δ*cruF* (FG/ΔG/Δ*crtR*/Δ*cruF*) strains of *Synechocystis*. (B) The presence of the FLAG-ChlG (F.ChlG) bait, HliD and Ycf39 was confirmed by immunoblotting with specific primary antibodies. (C) Anti-HliD

immunoblot of thylakoid membranes (30 µg of chlorophyll was loaded in each lane) from WT and mutant strains. (D) Absorbance spectra of the FG/ΔG (green), FG/ΔG/Δ*crtR* (red), FG/ΔG/Δ*cruF* (orange) and FG/ΔG/Δ*crtR/*Δ*cruF* (blue) eluates. (E) Separation of pigments extracted from immunoprecipitation eluates by RP-HPLC analysis monitoring absorbance at 450 nm. Myxoxanthophyll (Myx), zeaxanthin (Zea), 3-dehydroxy-myxoxanthophyll (D-Myx), chlorophyll *a* (Chl), echinenone (Ech) and β-carotene (β-car). In (A-E) data are representative of at least three independent experiments. (F) Quantification of F.ChlG, HliD and Ycf39 in immunoprecipitation eluates by mass spectrometry. The ion intensities shown in Table S2 were used to determine the ratios of HliD and Ycf39 to F.ChlG. The results of three technical repeats are presented with P values derived from a Student's t-test (paired, 2-tails).

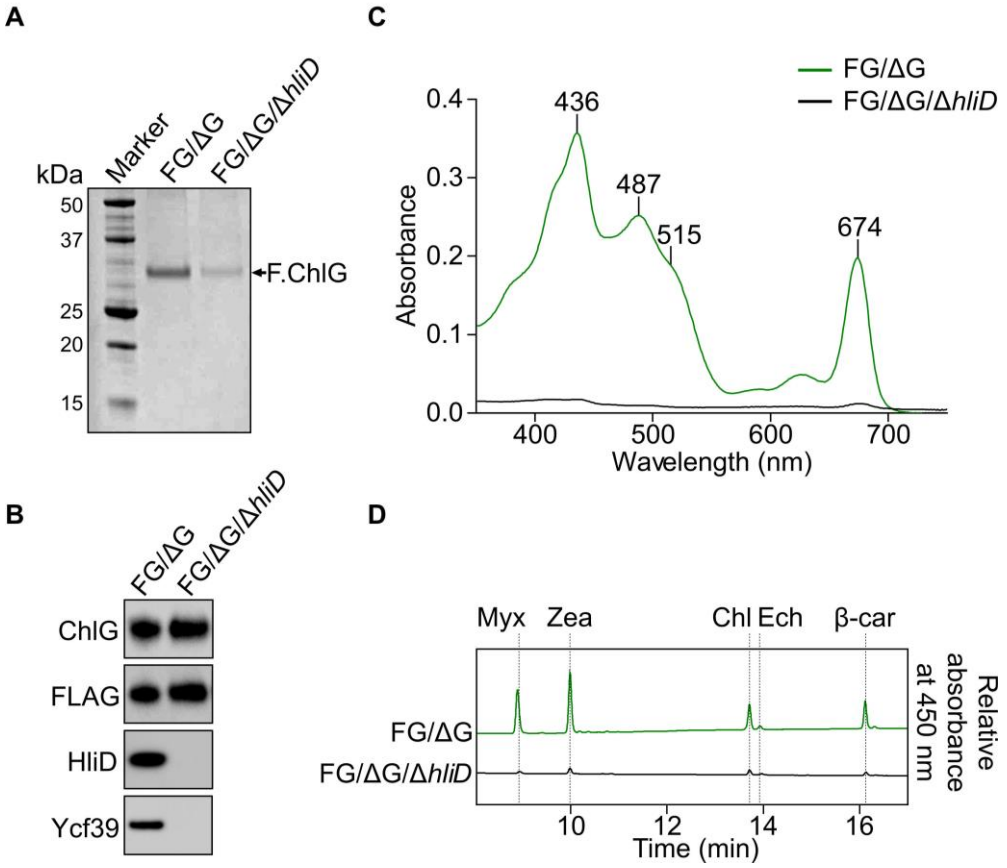

Figure 3. Analysis of pigment-protein complexes isolated by co-immunoprecipitation of F.ChlG from a *Synechocystis* Δ*hliD* mutant. (A) Coomassie stained SDS-PAGE analysis of FLAG immunoprecipitation eluates obtained from the FLAG-*chlG* Δ*chlG* (FG/ΔG) and FLAG-*chlG* Δ*chlG* Δ*hliD* (FG/ΔG/Δ*hliD*) strains. (B) The presence of the FLAG-ChlG (F.ChlG) bait, HliD and Ycf39 was identified by immunoblotting with specific primary antibodies. The FG/ΔG/Δ*hliD* protein concentration was normalised to that of FG/ΔG. (C) Absorbance spectra of the FG/ΔG (green) and FG/ΔG/Δ*hliD* (black) eluates. (D) Separation of pigments extracted from immunoprecipitation eluates by RP-HPLC analysis monitoring absorbance at 450 nm. Myxoxanthophyll (Myx), zeaxanthin (Zea), 3-dehydroxy-myxoxanthophyll (D-Myx), chlorophyll *a* (Chl), echinenone (Ech) and β-carotene (β-car). Data are representative of at least three independent experiments.

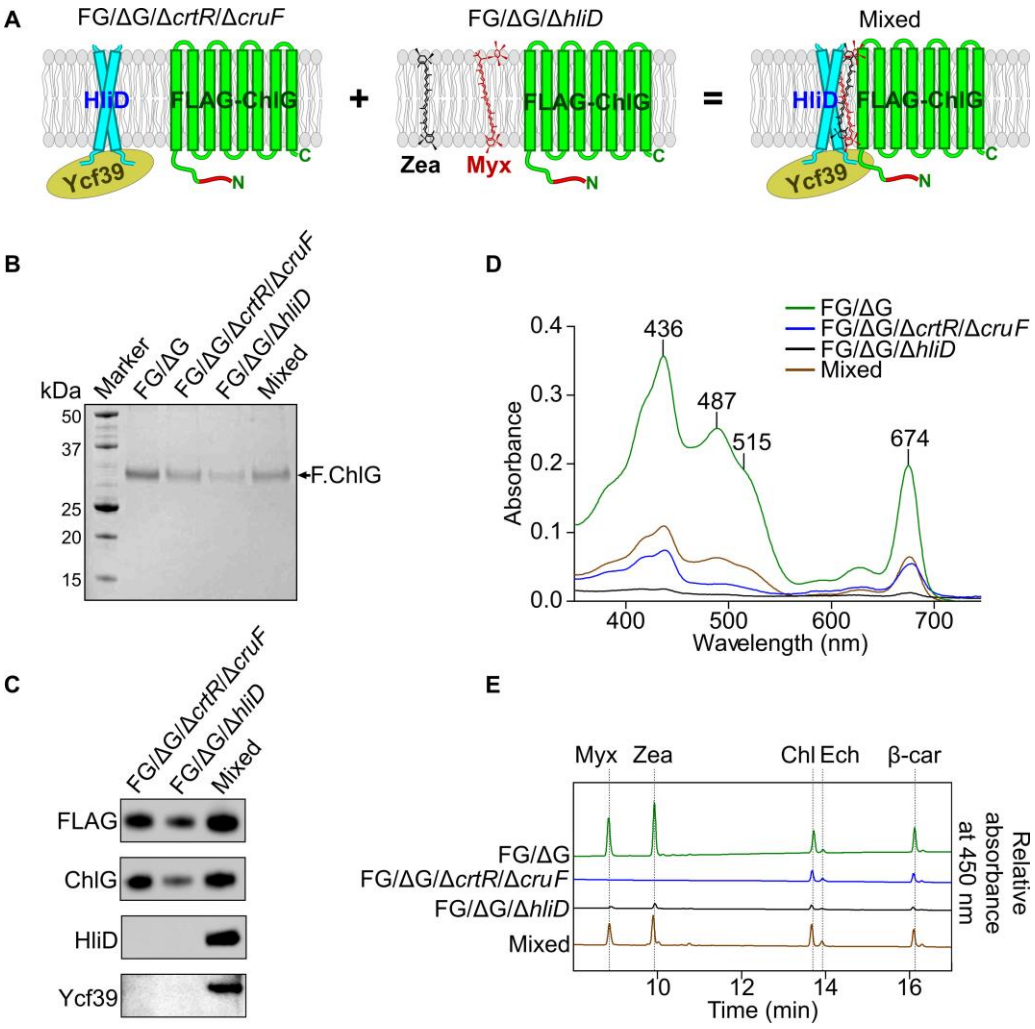

Figure 4. Reconstitution of F.ChlG with carotenoids and HliD in isolated membranes. (A) Solubilised thylakoid membranes from the FLAG-*chlG* Δ*chlG* strain lacking zeaxanthin and myxoxanthophyll (FG/ΔG/Δ*crtR*/Δ*cruF*) but containing FLAG-ChlG (green) and HliD (blue) were mixed with membranes from the FG/ΔG/Δ*hliD* strain, which lacks HliD but contains myxoxanthophyll (Myx, red) and zeaxanthin (Zea, black). (B) Analysis of FLAG immunoprecipitants by SDS-PAGE and Coomassie blue staining; the mixed membranes are labelled as 'Mixed'. (C) Immunodetection of FLAG-ChlG (F.ChlG), HliD and Ycf39 in the immunoprecipitation eluates. HliD and Ycf39 are restored in the mixed membrane sample. (D) Absorbance spectra of each immunoprecipitation eluate. (E) Qualitative RP-HPLC identification of myxoxanthophyll (Myx), zeaxanthin (Zea), chlorophyll *a* (Chl) echinenone (Ech) and β-carotene (β-car). Data are representative of at least three independent experiments.

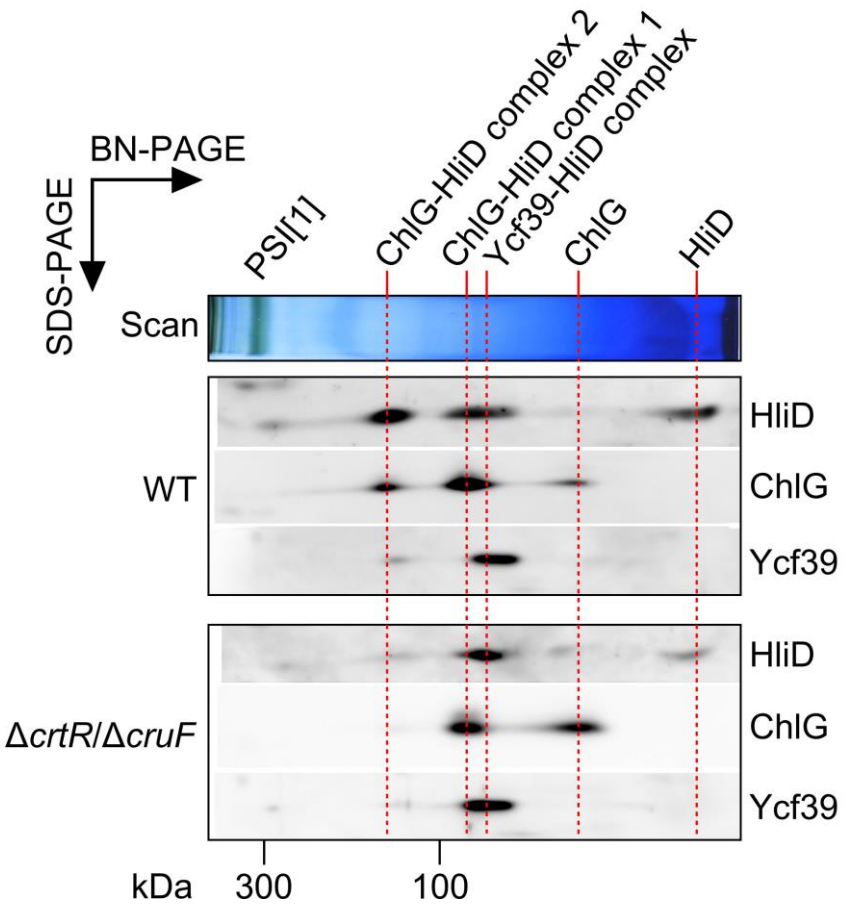

Figure 5. Formation of ChlG-HliD complexes is altered by the loss of zeaxanthin and myxoxanthophyll. Analysis of thylakoid membrane proteins by 2D-PAGE and immunoblotting. Thylakoid membranes were purified from WT and Δ*crtR/*Δ*cruF* cells and separated by BN-PAGE in the first dimension and denaturing SDS-PAGE in the second dimension. Proteins were transferred to a PVDF membrane and immunodetection of ChlG, HliD and Ycf39 was performed using protein specific primary antibodies. Proteins and protein complexes assigned according to previous studies (28, 30) are indicated with red dashed lines and labelled above the gel slice/blots. The approximate molecular weight is indicated below the blots.

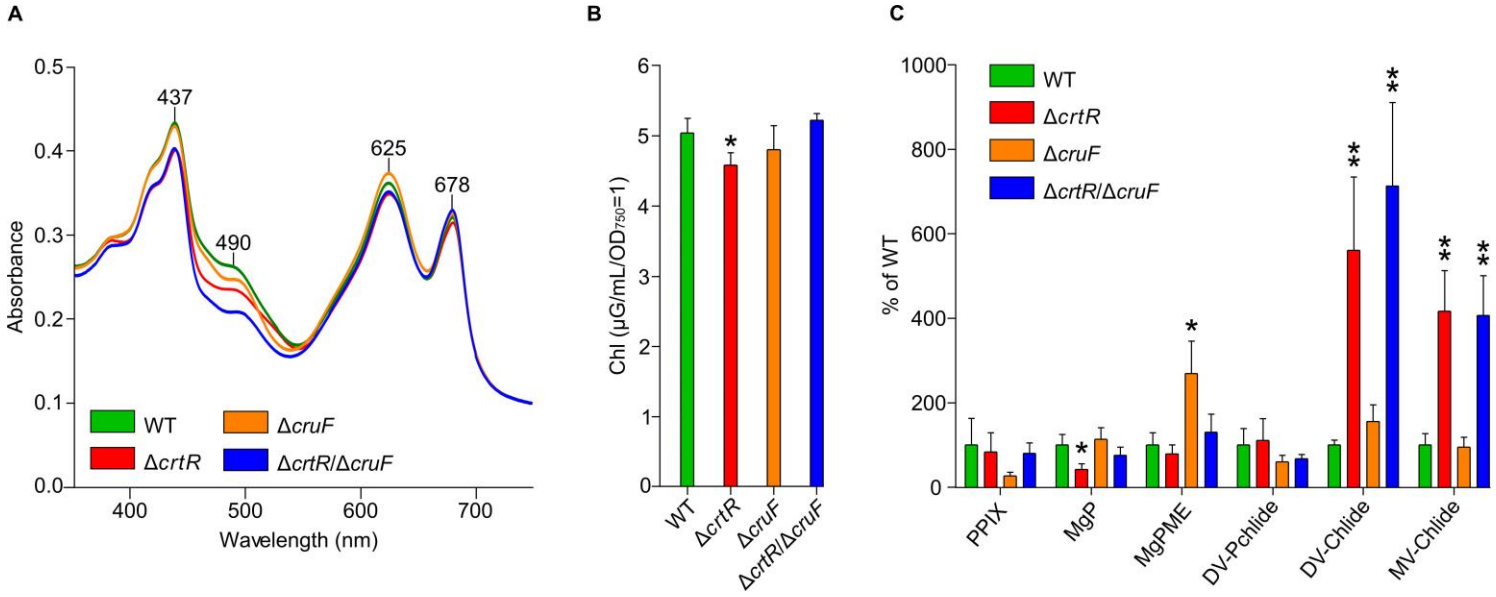

Figure 6. Quantification of Chl and Chl precursors in wild-type *Synechocystis* and xanthophyll deficient mutants. (A) Whole cell absorbance spectra of wild-type (WT, green), Δ*crtR* (red), Δ*cruF* (orange) and Δ*crtR*/Δ*cruF* (blue). (B) Chl content of each strain. Error bars represent the standard deviation from the mean of 5 biological replicates. (C) Levels of Chl precursors extracted from Δ*crtR*, Δ*cruF* and Δ*crtR*/Δ*cruF* cells, relative to those in the WT, which was set at 100% for each pigment. PPIX = protoporphyrin IX; MgP = magnesium-protoporphyrin IX; MgPME = magnesium protoporphyrin monomethyl ester; DV-Pchlide = divinyl-protochlorophyllide; DV-Chlide = divinyl-chlorophyllide; MV-Chlide = monovinyl-chlorophyllide. Error bars represent the standard deviation from the mean of 5 biological replicates. In (B) and (C) statistical significance between the means for Chl/each precursor was determined using one-way analysis of variance (ANOVA); * = $p < 0.05$; ** = $p < 0.001$.

A

chlorophyllide *a*

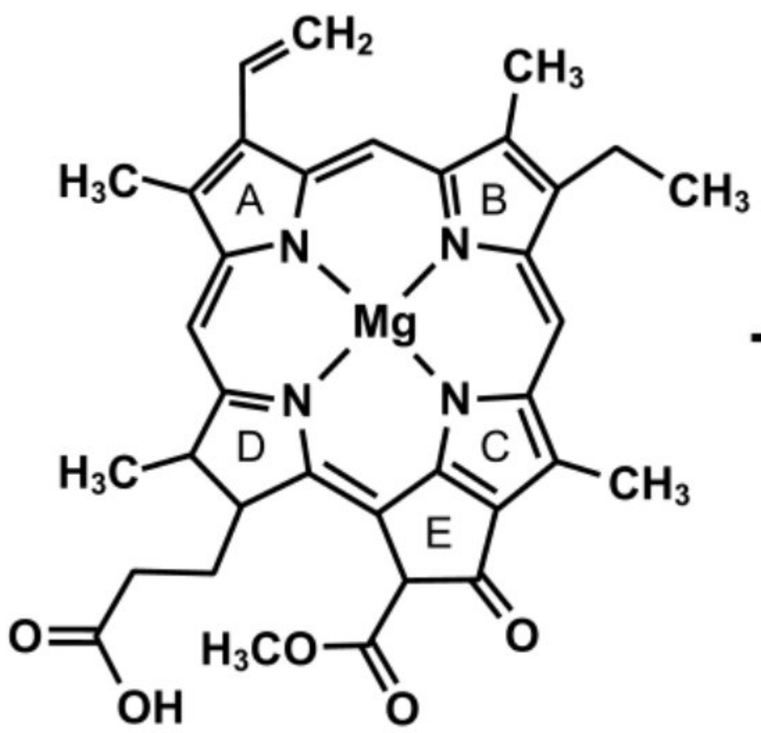

GGPP
or PPP

ChlG

chlorophyll *a*

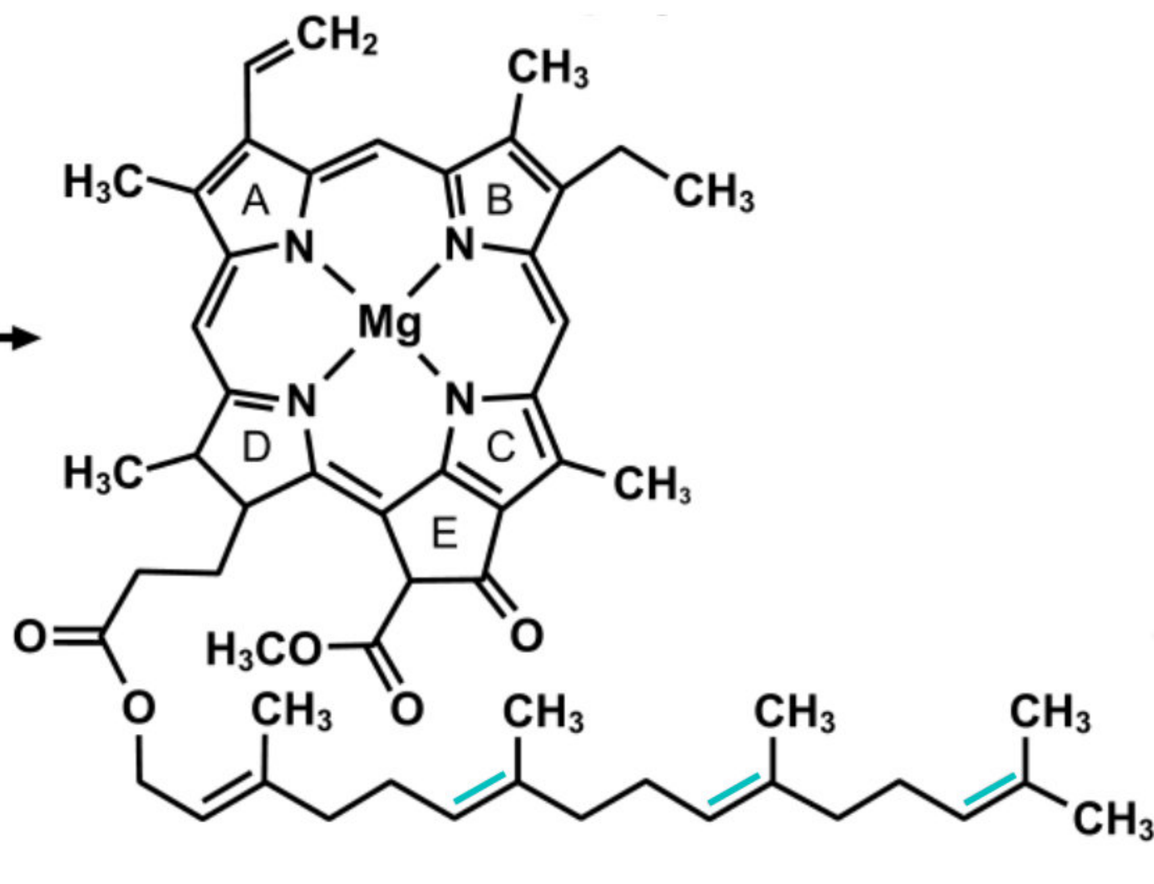

B

β-carotene

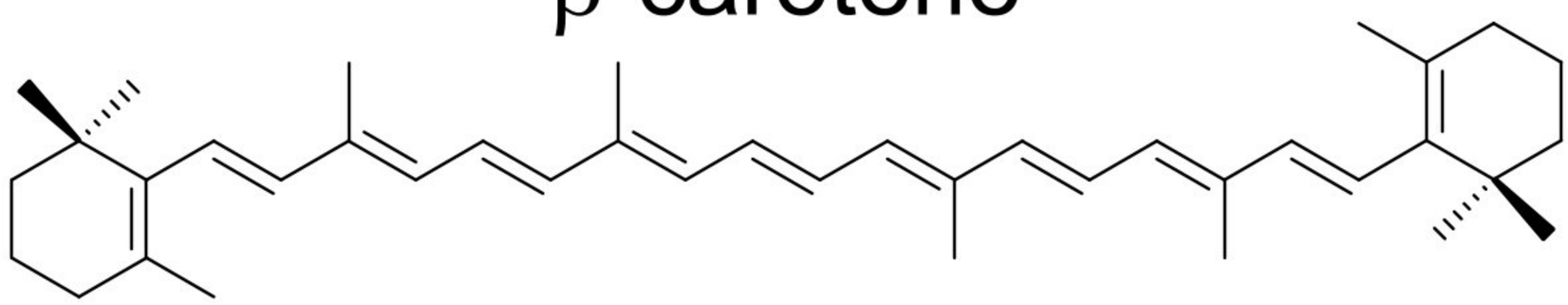

zeaxanthin

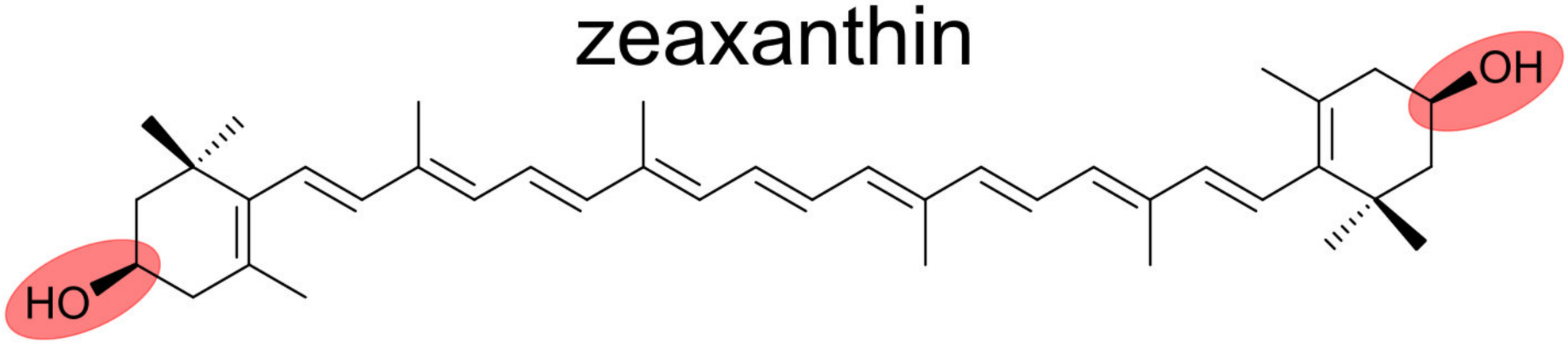

echinenone

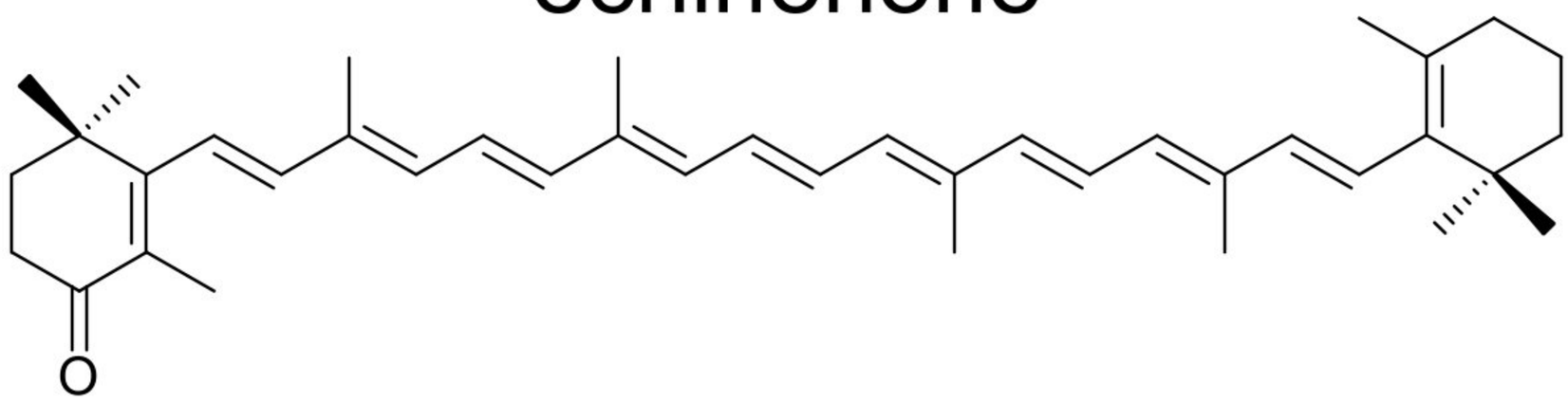

myxoxanthophyll

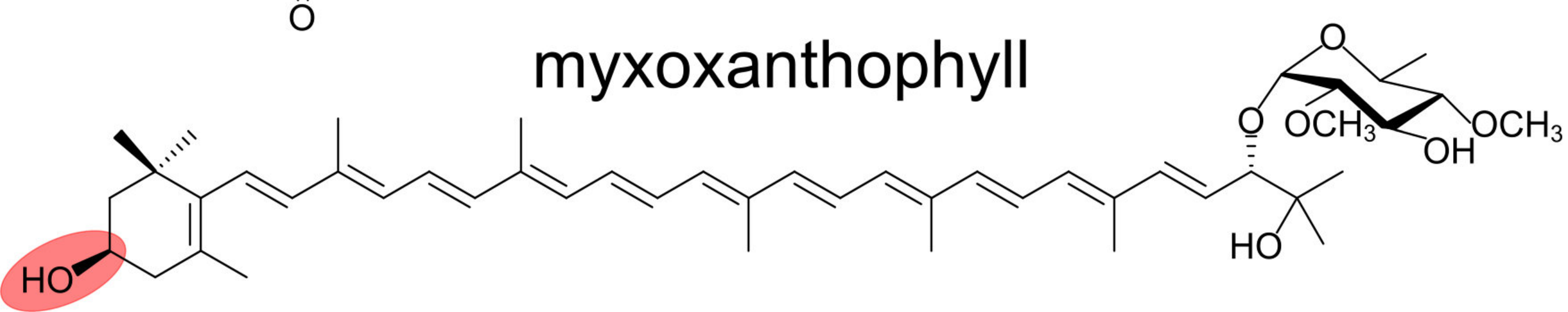

A

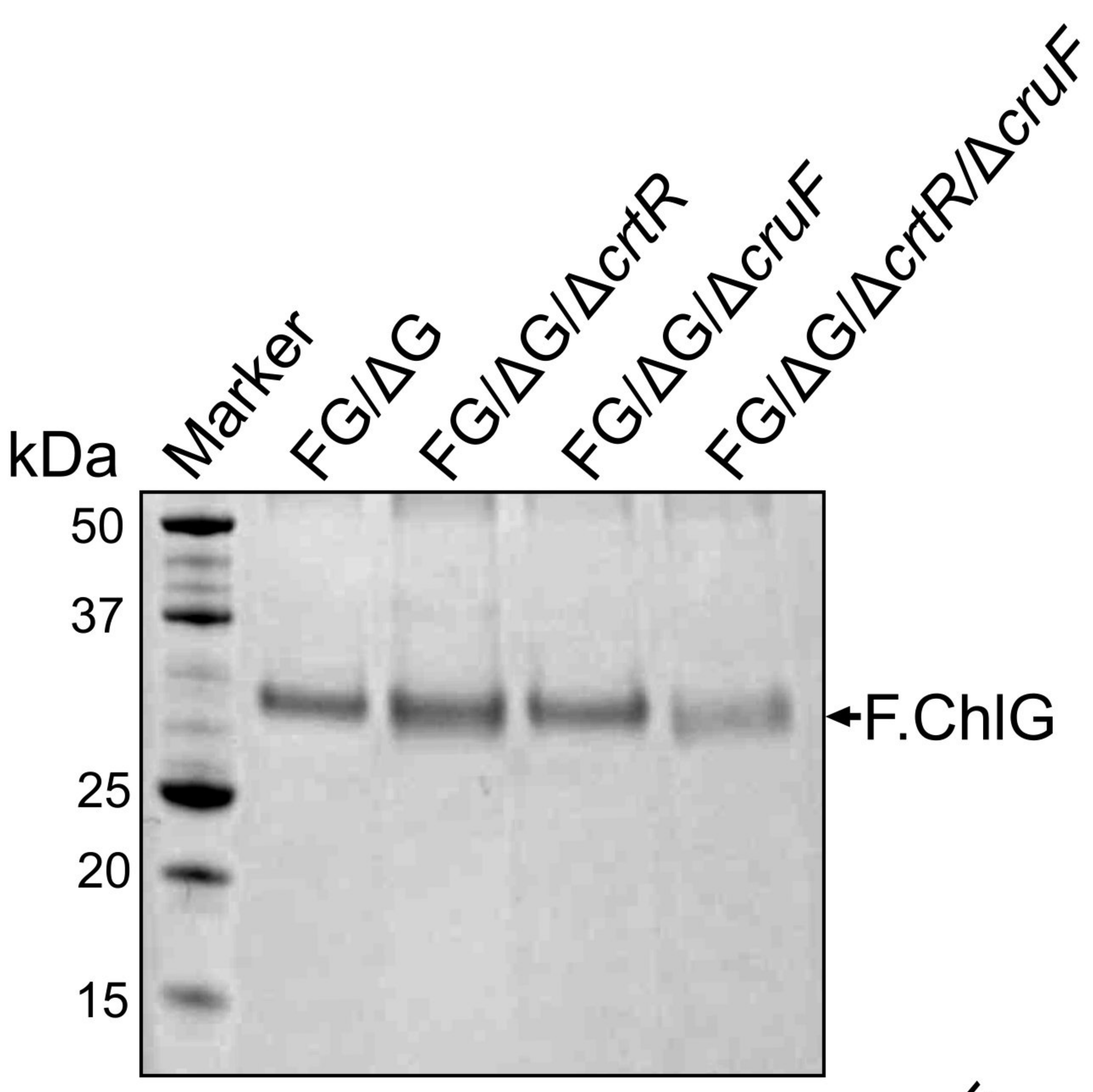
Marker
FG/ΔG
FG/ΔG/ΔcrtR
FG/ΔG/ΔcruF
FG/ΔG/ΔcrtR/ΔcruF
kDa
50
37
25
20
15
F.ChlG

B

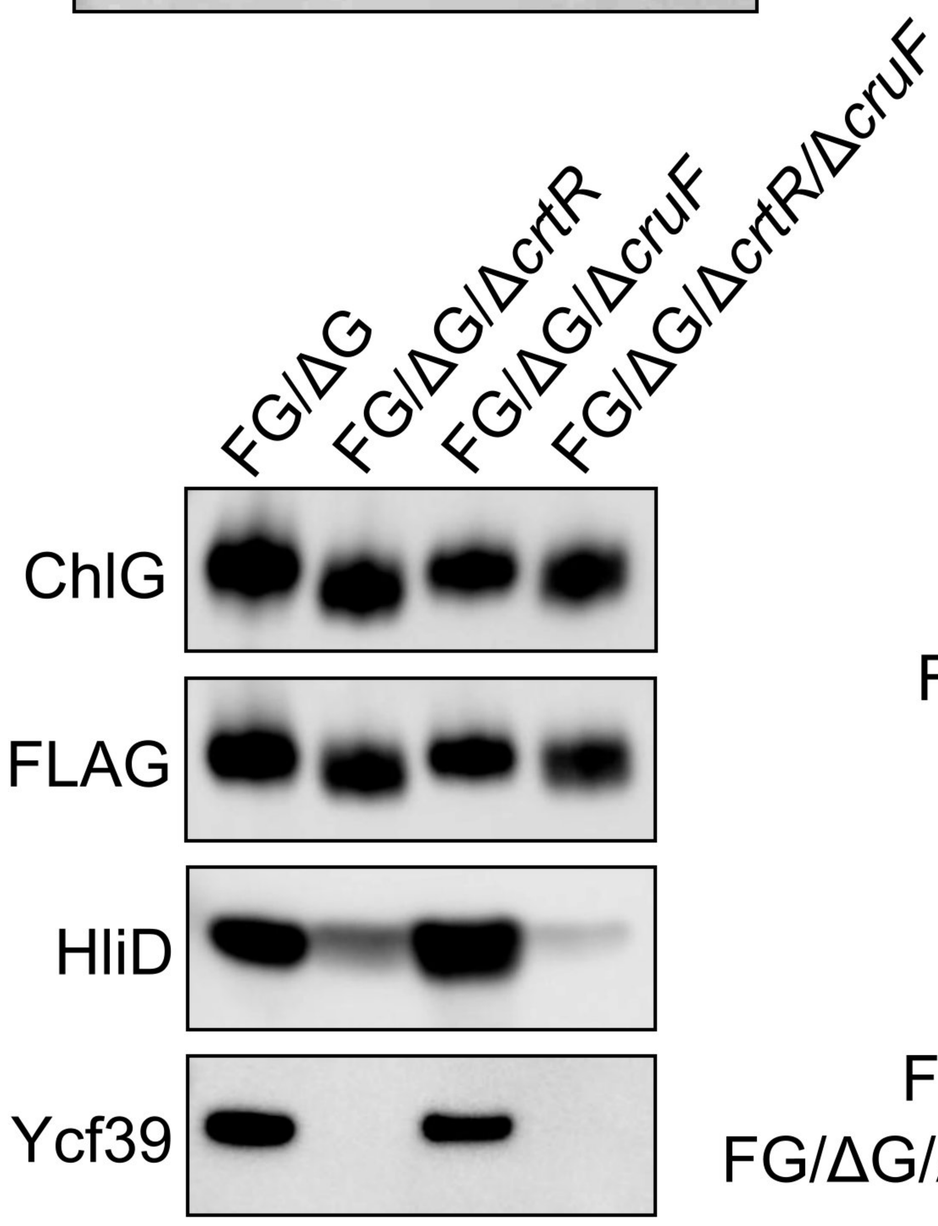
FG/ΔG
FG/ΔG/ΔcrtR
FG/ΔG/ΔcruF
FG/ΔG/ΔcrtR/ΔcruF
ChlG
FLAG
HliD
Ycf39

C

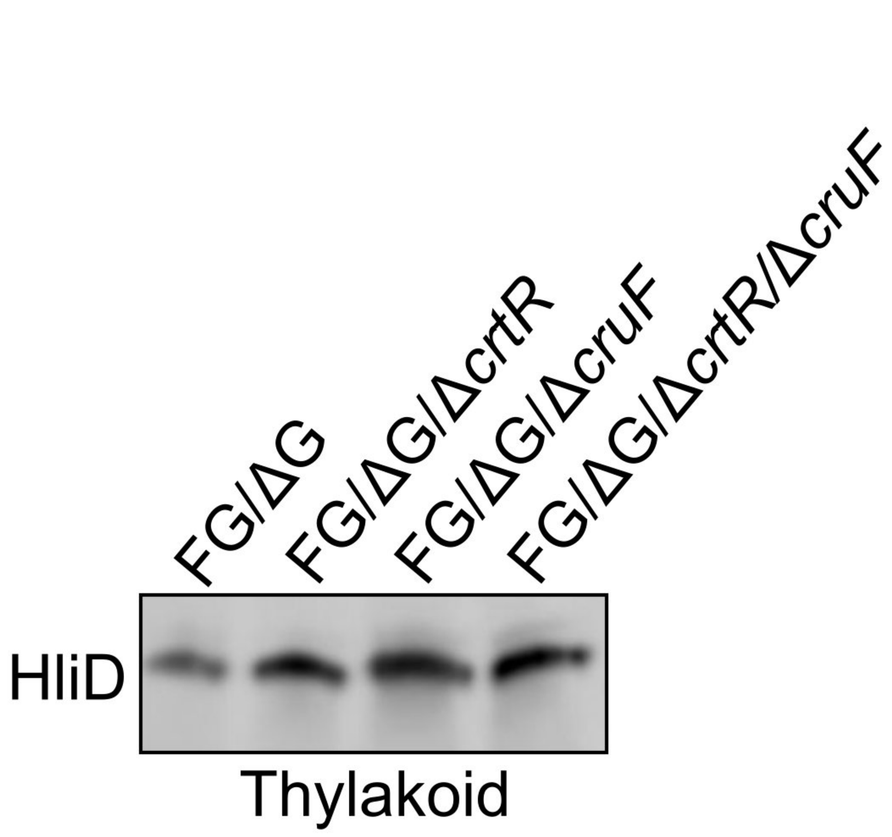
FG/ΔG
FG/ΔG/ΔcrtR
FG/ΔG/ΔcruF
FG/ΔG/ΔcrtR/ΔcruF
HliD
Thylakoid

D

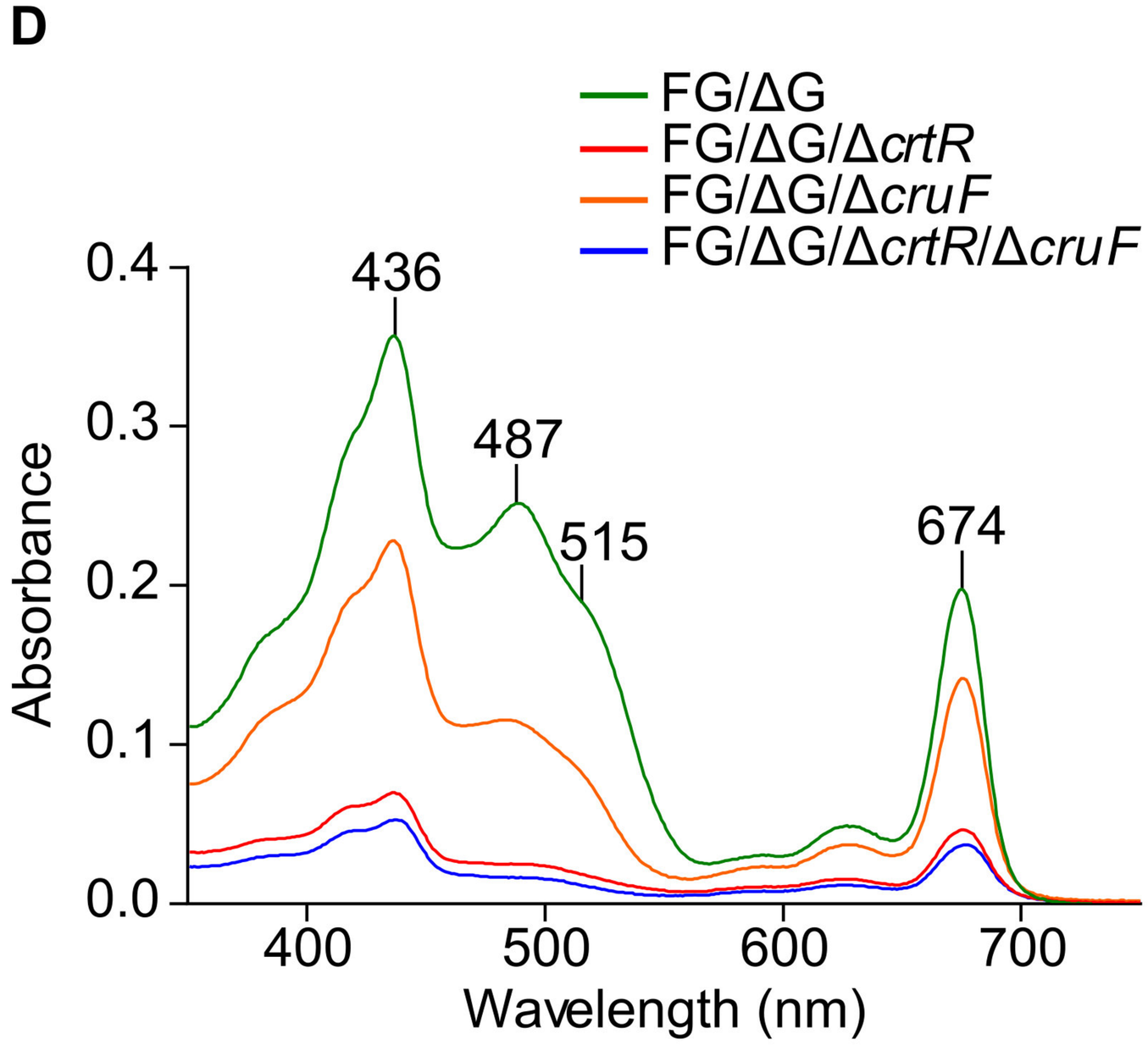
FG/ΔG
FG/ΔG/ΔcrtR
FG/ΔG/ΔcruF
FG/ΔG/ΔcrtR/ΔcruF
436
487
515
674
Absorbance
0.4
0.3
0.2
0.1
0.0
400
500
600
700
Wavelength (nm)

E

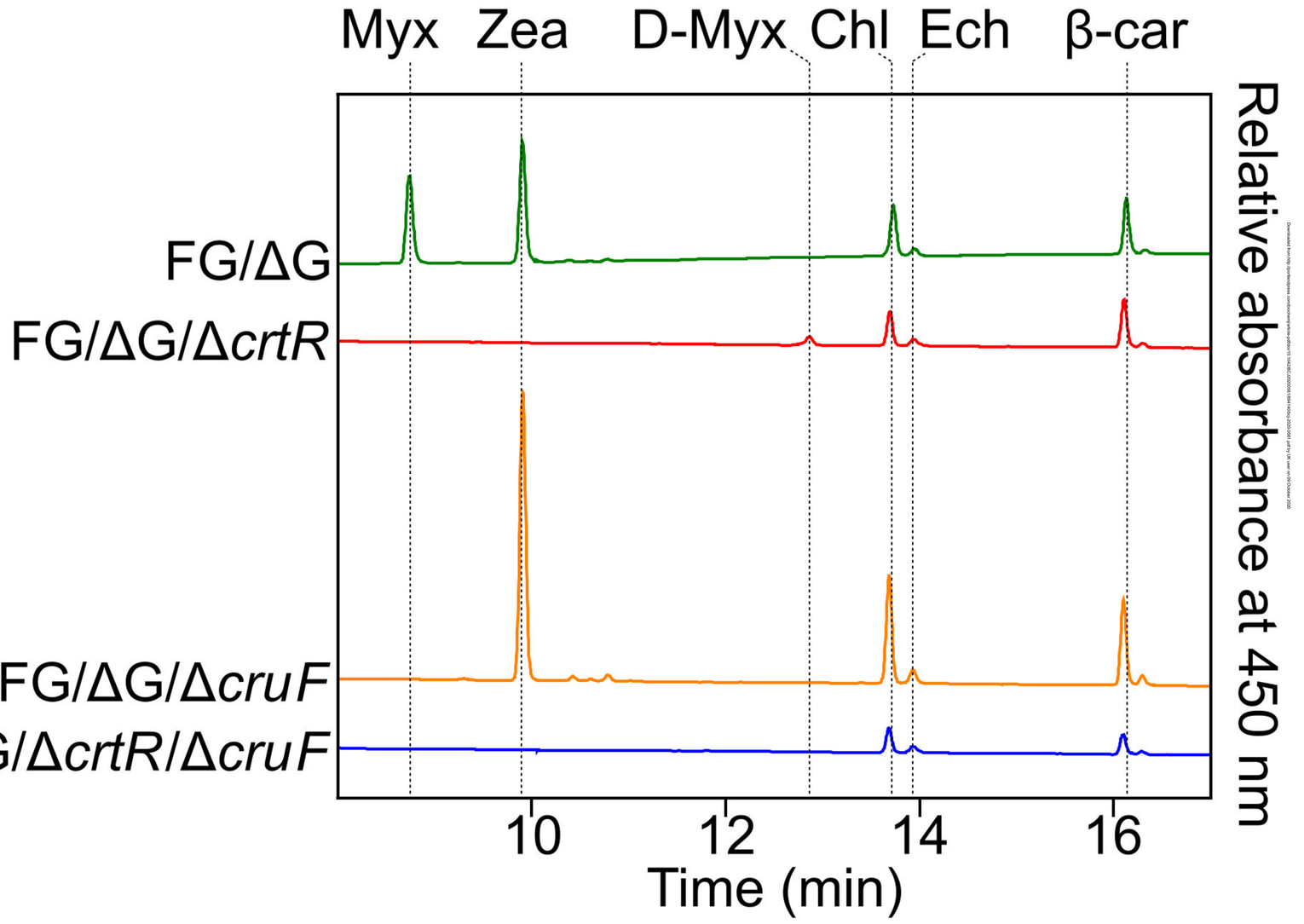
Myx
Zea
D-Myx
Chl
Ech
β-car
FG/ΔG
FG/ΔG/ΔcrtR
FG/ΔG/ΔcruF
FG/ΔG/ΔcrtR/ΔcruF
Relative absorbance at 450 nm
10
12
14
16
Time (min)

F

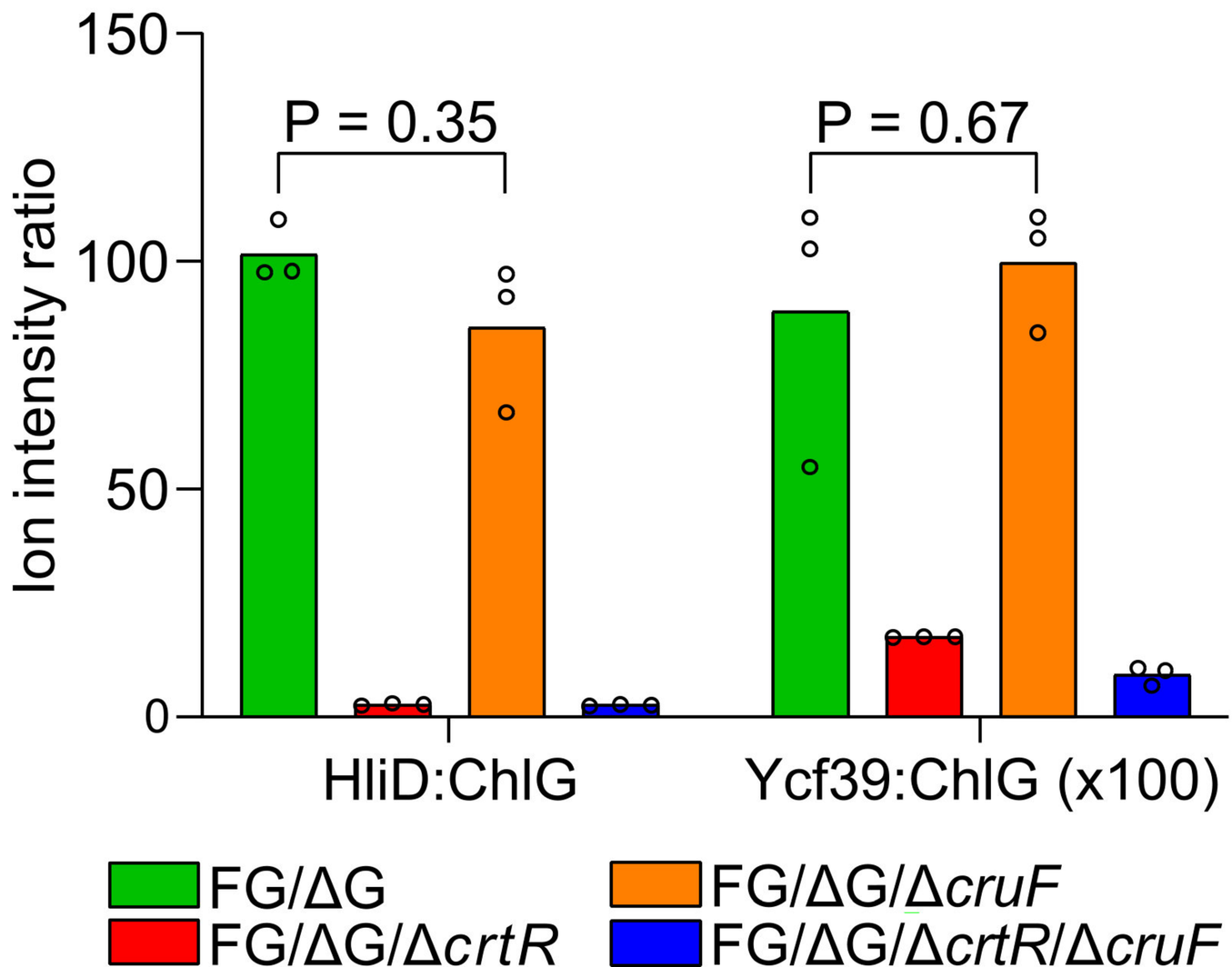
P = 0.35
P = 0.67
Ion intensity ratio
150
100
50
0
HliD:ChlG
Ycf39:ChlG (x100)
FG/ΔG
FG/ΔG/ΔcruF
FG/ΔG/ΔcrtR
FG/ΔG/ΔcrtR/ΔcruF

A

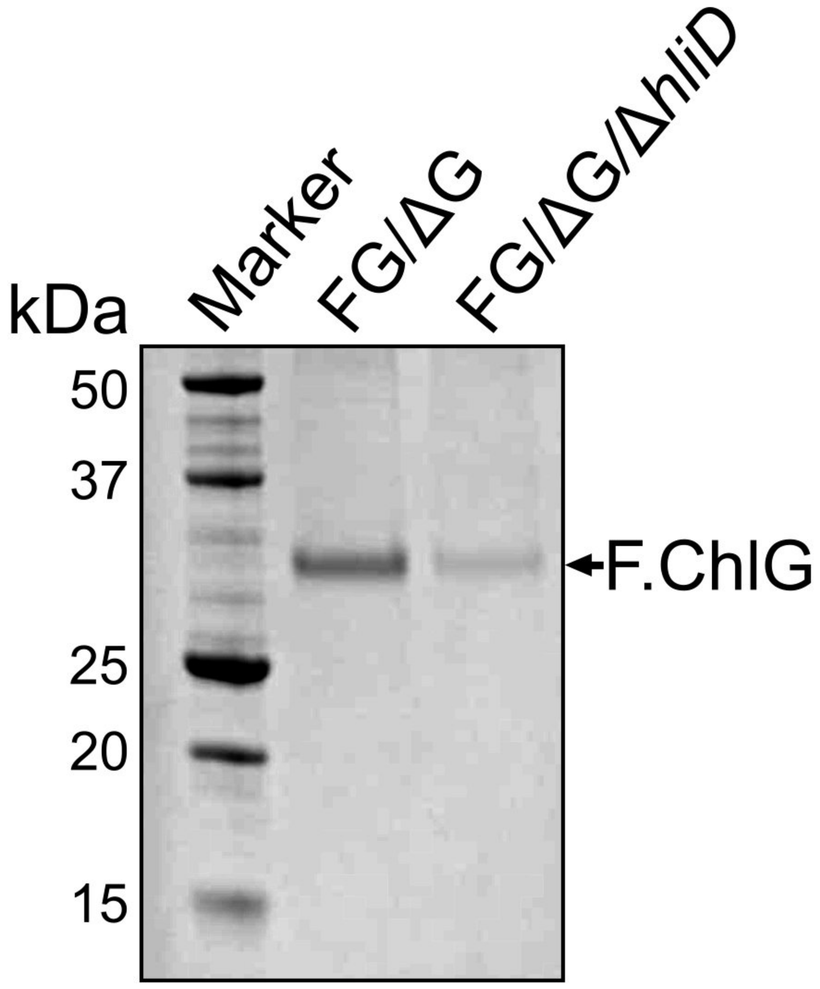
Marker
FG/ΔG
FG/ΔG/ΔhliD
kDa
50
37
25
20
15
F.ChlG

B

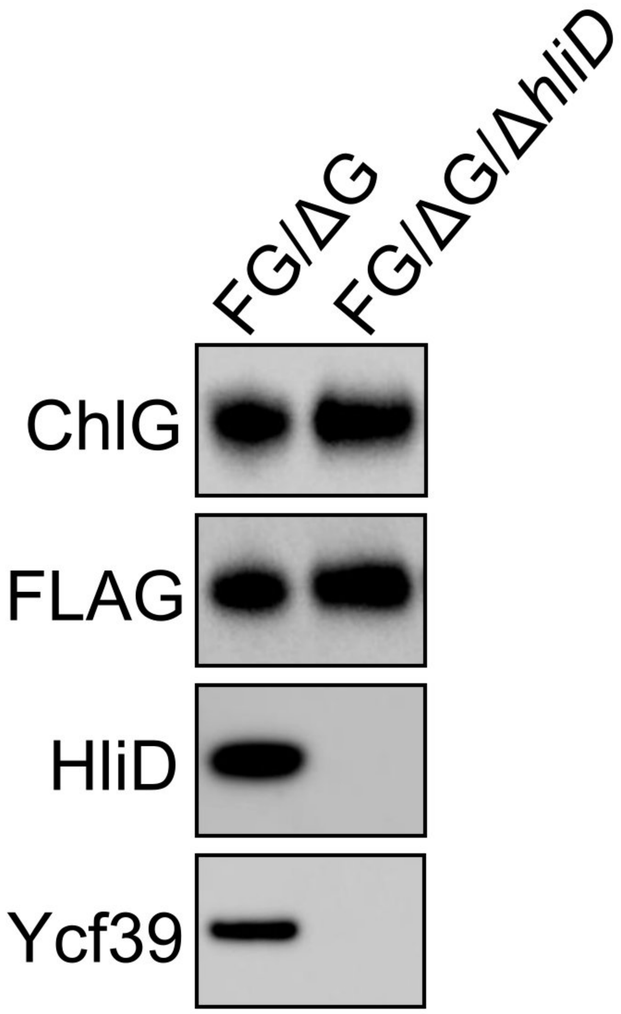
FG/ΔG
FG/ΔG/ΔhliD
ChlG
FLAG
HliD
Ycf39

C

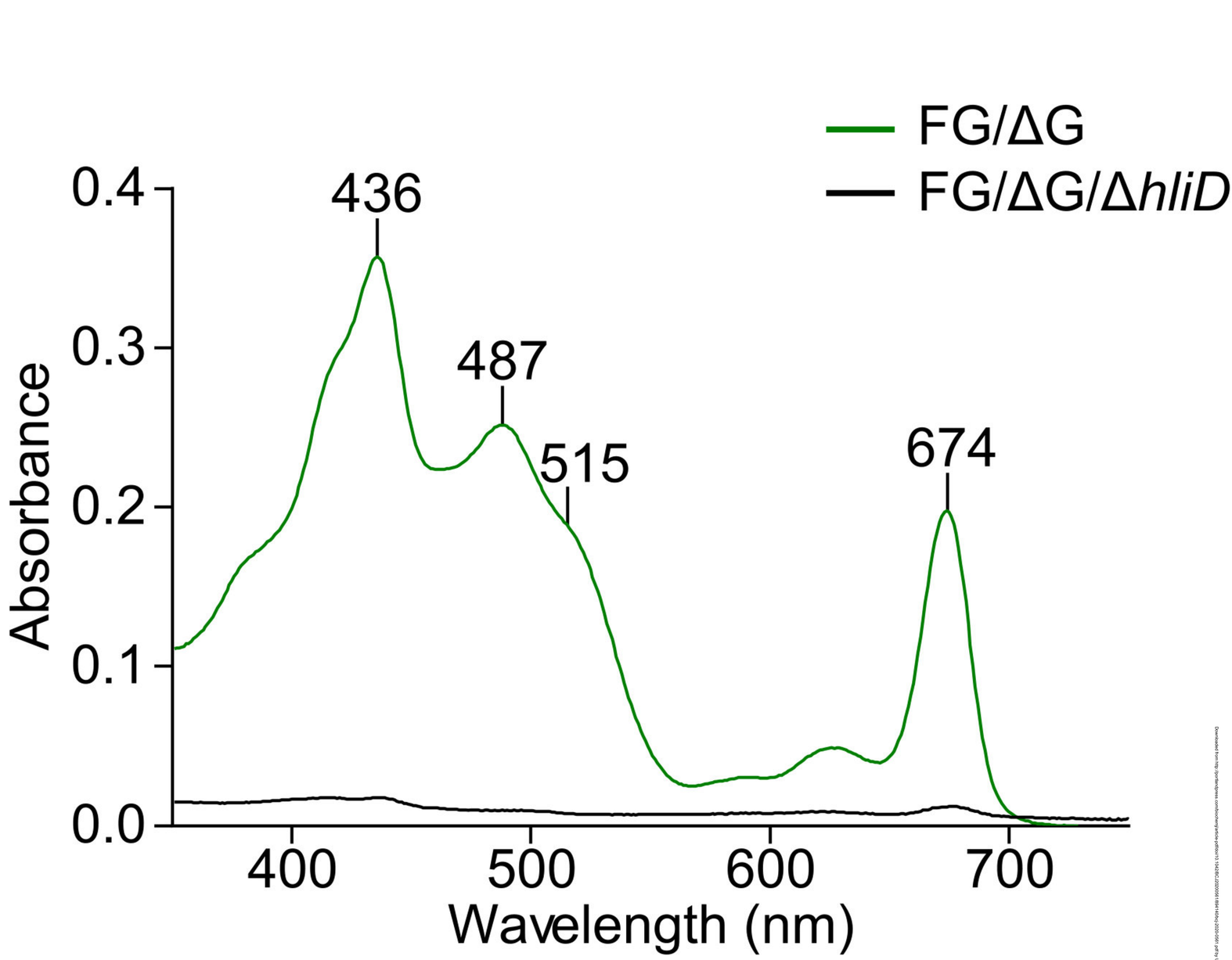
FG/ΔG
FG/ΔG/ΔhliD
436
487
515
674
Absorbance
0.4
0.3
0.2
0.1
0.0
400
500
600
700
Wavelength (nm)

D

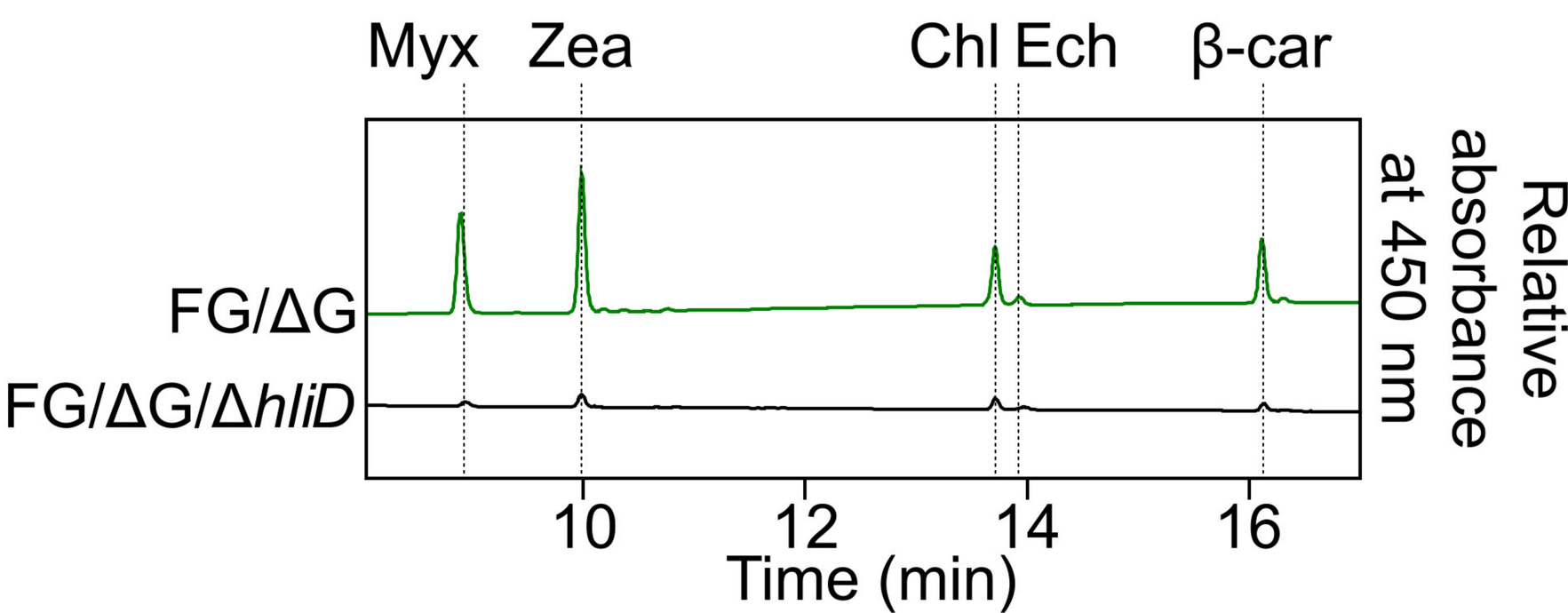
Myx
Zea
Chl
Ech
β-car
FG/ΔG
FG/ΔG/ΔhliD
Relative absorbance at 450 nm
10
12
14
16
Time (min)

A

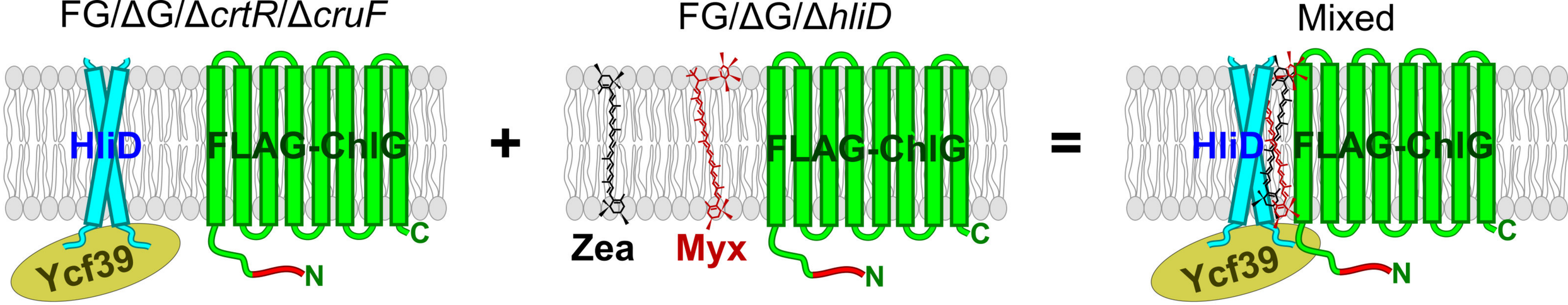
FG/ΔG/ΔcrtR/ΔcruF
HliD
FLAG-ChlG
C
N
Ycf39
+
FG/ΔG/ΔhliD
Zea
Myx
FLAG-ChlG
C
N
=
Mixed
HliD
FLAG-ChlG
C
N
Ycf39

B

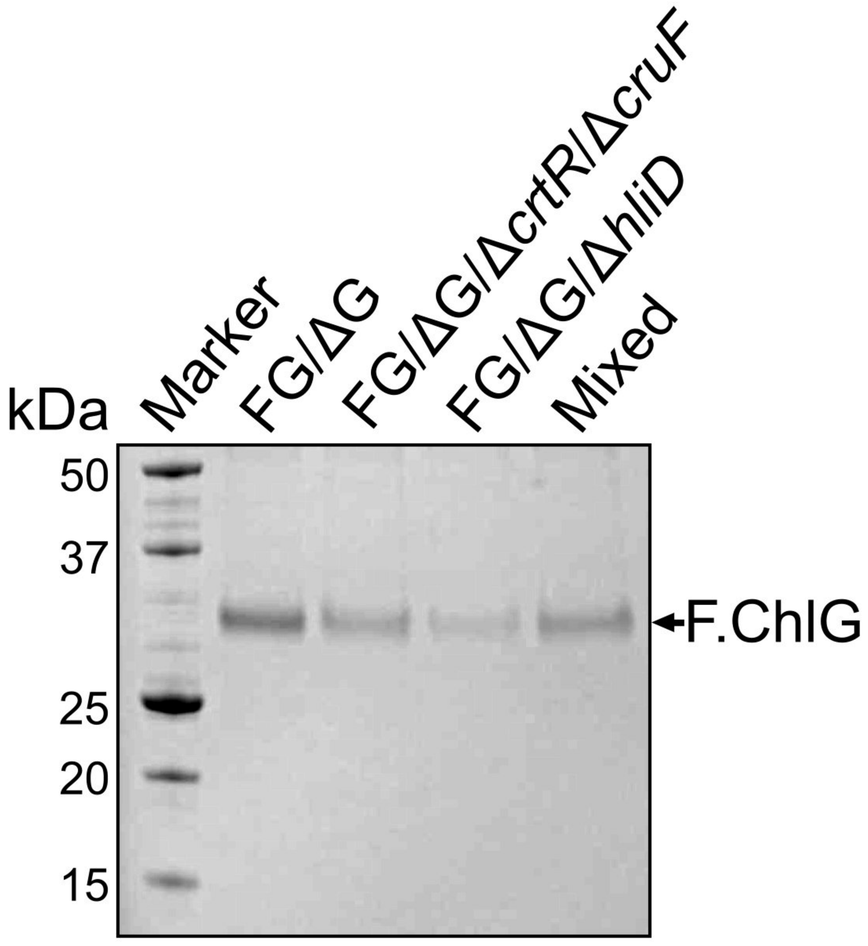
kDa
Marker
FG/ΔG
FG/ΔG/ΔcrtR/ΔcruF
FG/ΔG/ΔhliD
Mixed
50
37
25
20
15
F.ChlG

C

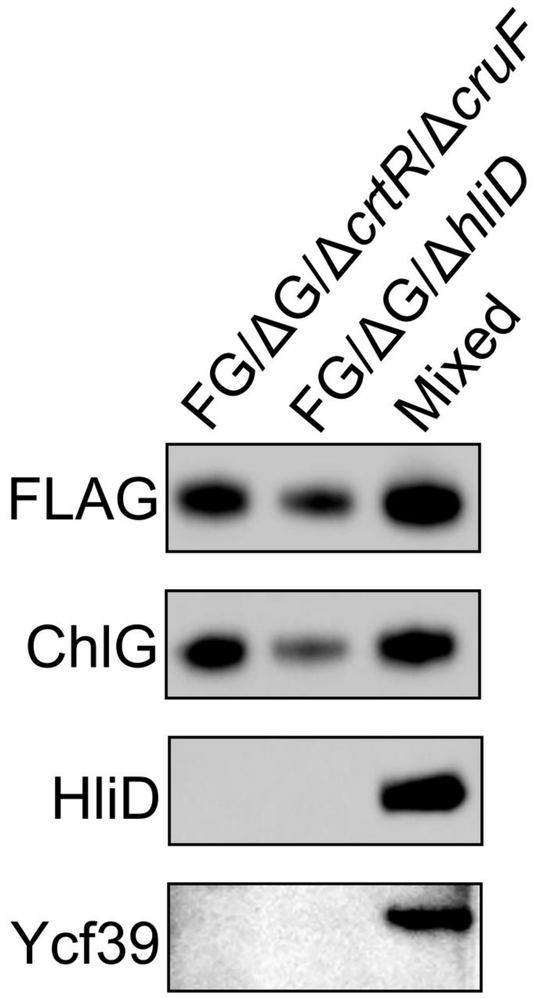
FG/ΔG/ΔcrtR/ΔcruF
FG/ΔG/ΔhliD
Mixed
FLAG
ChlG
HliD
Ycf39

D

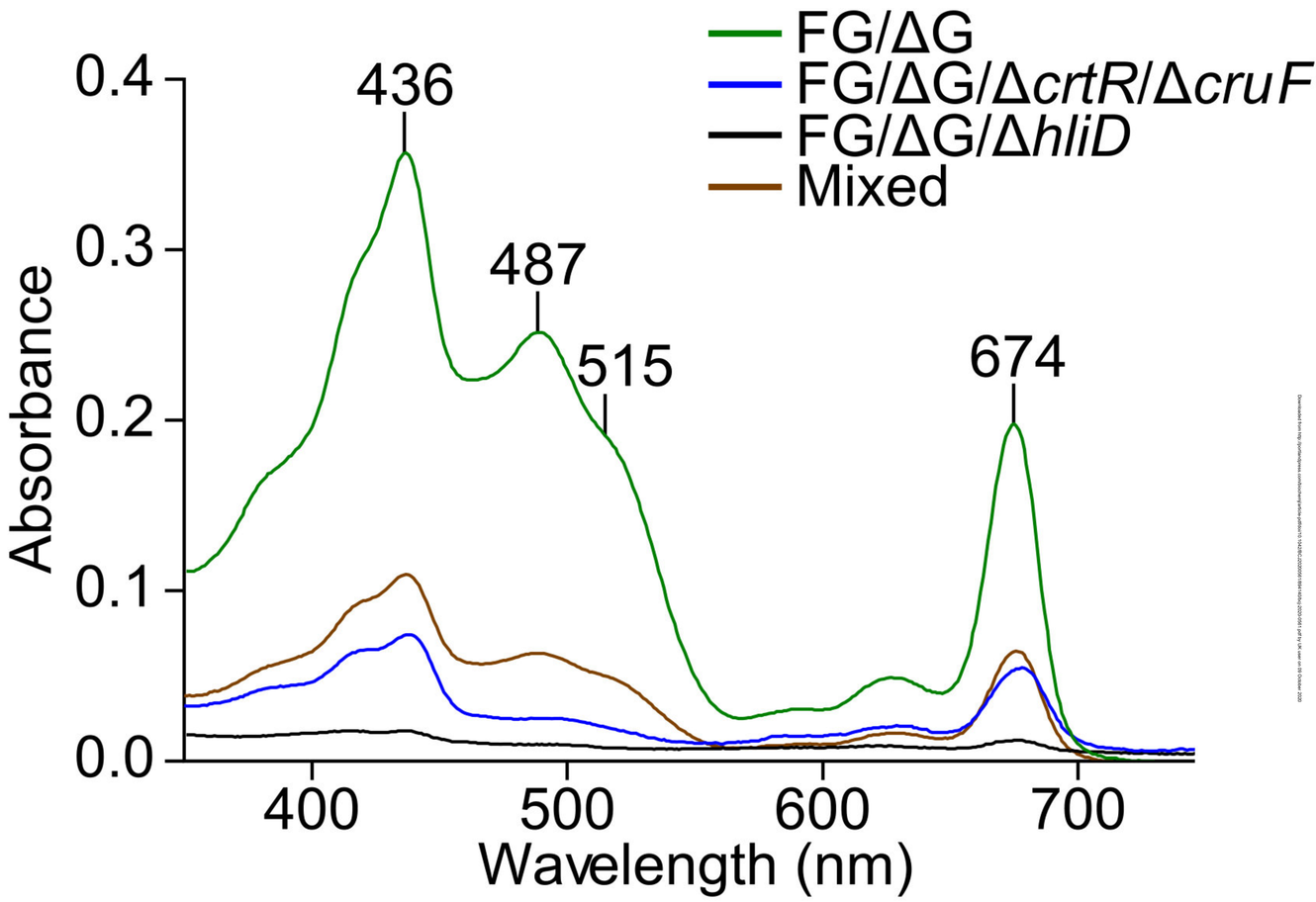
FG/ΔG
FG/ΔG/ΔcrtR/ΔcruF
FG/ΔG/ΔhliD
Mixed
436
487
515
674
Absorbance
0.4
0.3
0.2
0.1
0.0
400
500
600
700
Wavelength (nm)

E

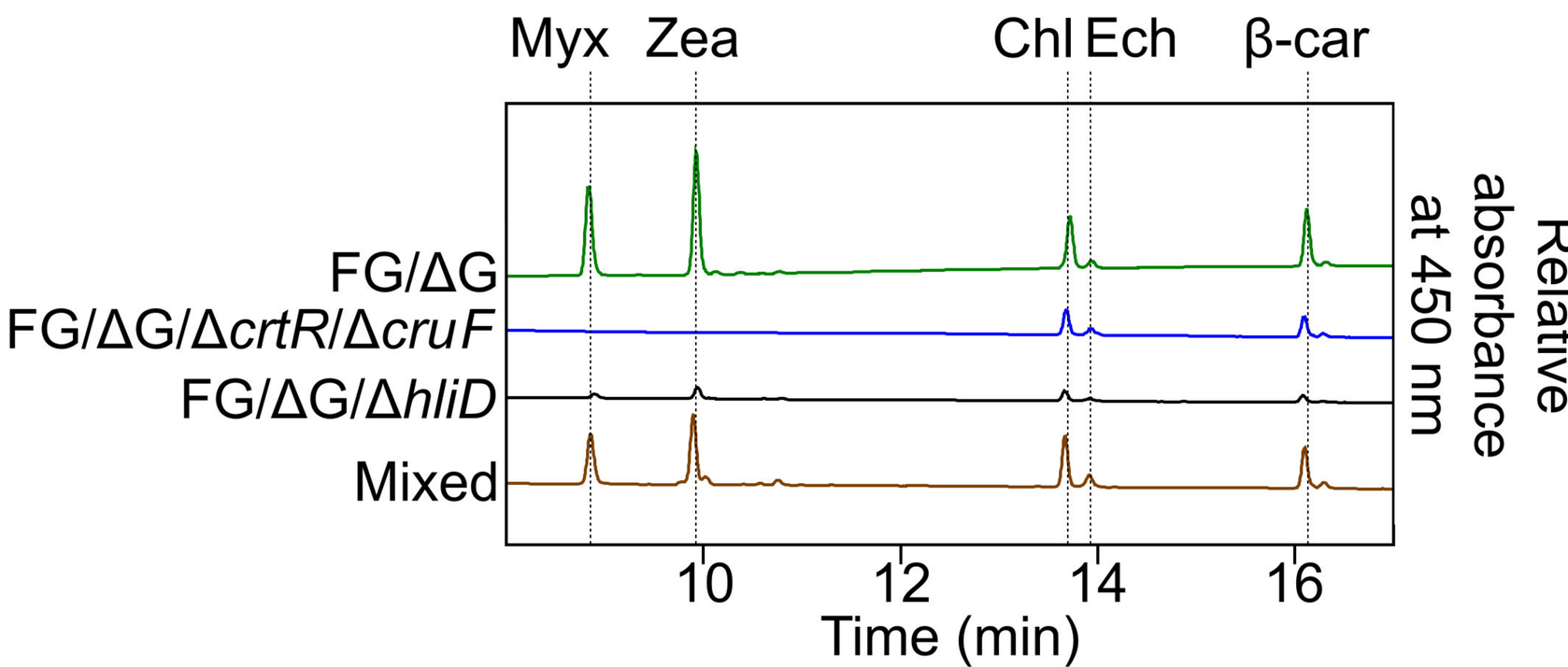
Myx
Zea
Chl
Ech
β-car
FG/ΔG
FG/ΔG/ΔcrtR/ΔcruF
FG/ΔG/ΔhliD
Mixed
10
12
14
16
Time (min)
Relative absorbance at 450 nm

BN-PAGE

SDS-PAGE

PSI[1]

ChlG-HliD complex 2

ChlG-HliD complex 1

Ycf39-HliD complex

ChlG

HliD

Scan

HliD

WT

ChlG

Ycf39

HliD

Δ*crtR*/Δ*cruF*

ChlG

Ycf39

kDa

300

100

A

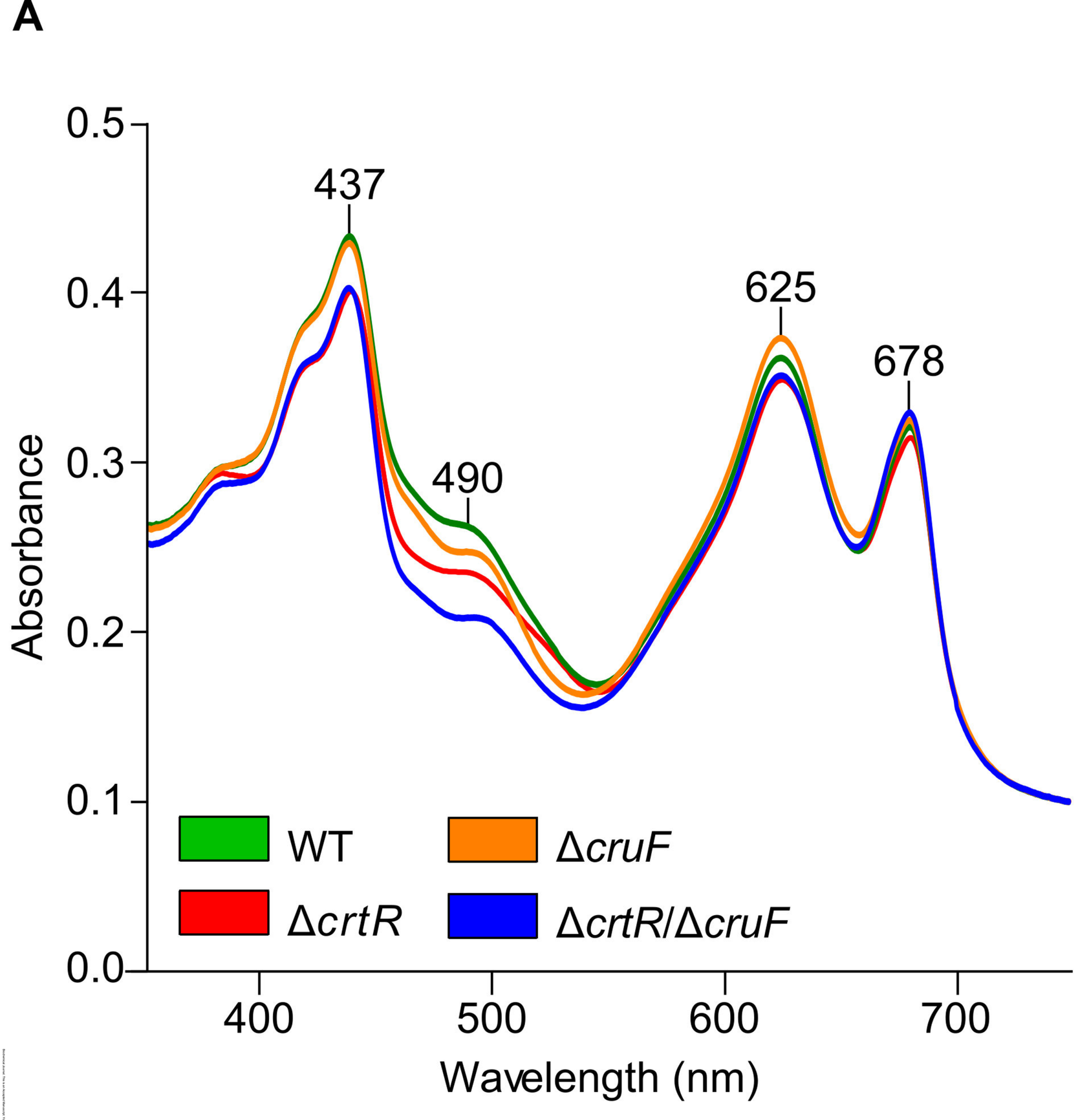
0.5
0.4
0.3
0.2
0.1
0.0
Absorbance
437
490
625
678
WT
ΔcruF
ΔcrtR
ΔcrtR/ΔcruF
400
500
600
700
Wavelength (nm)

B

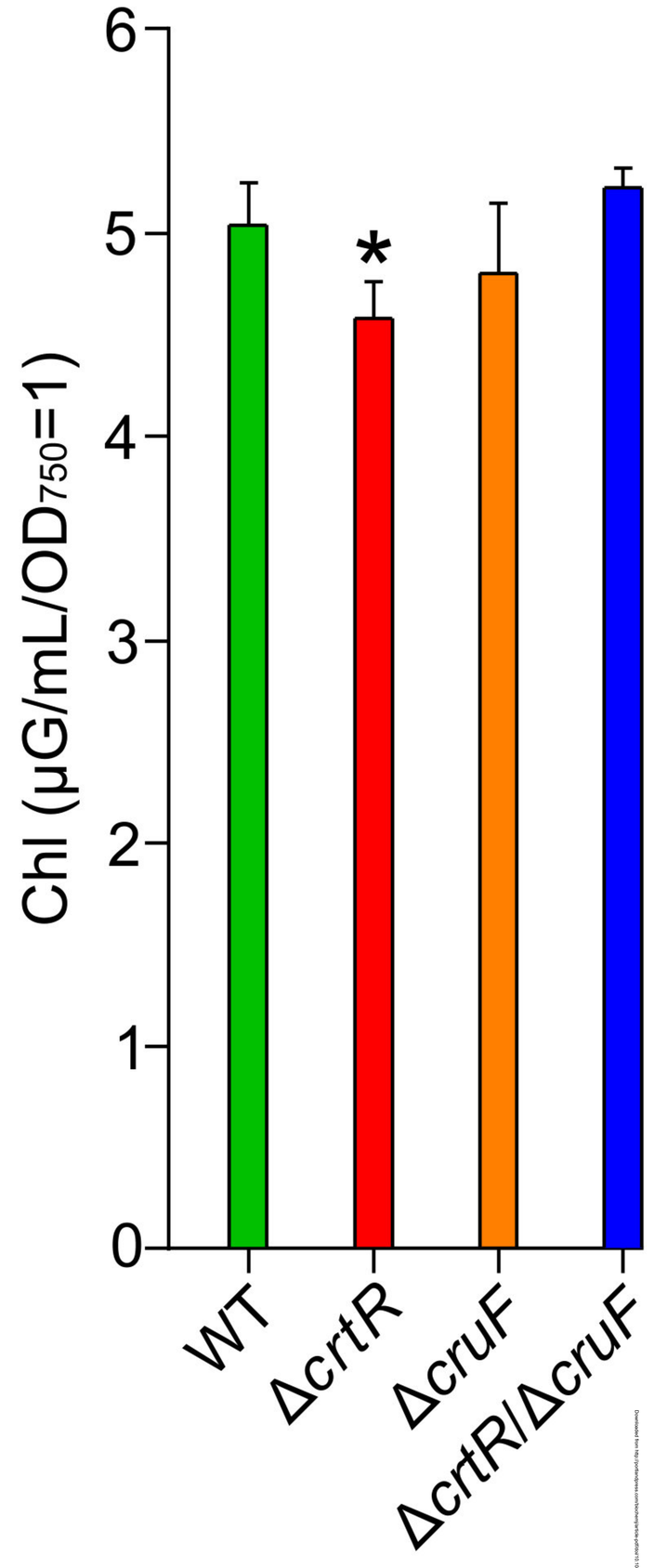
6
5
4
3
2
1
0
Chl (μG/mL/OD750=1)
*
WT
ΔcrtR
ΔcruF
ΔcrtR/ΔcruF

C

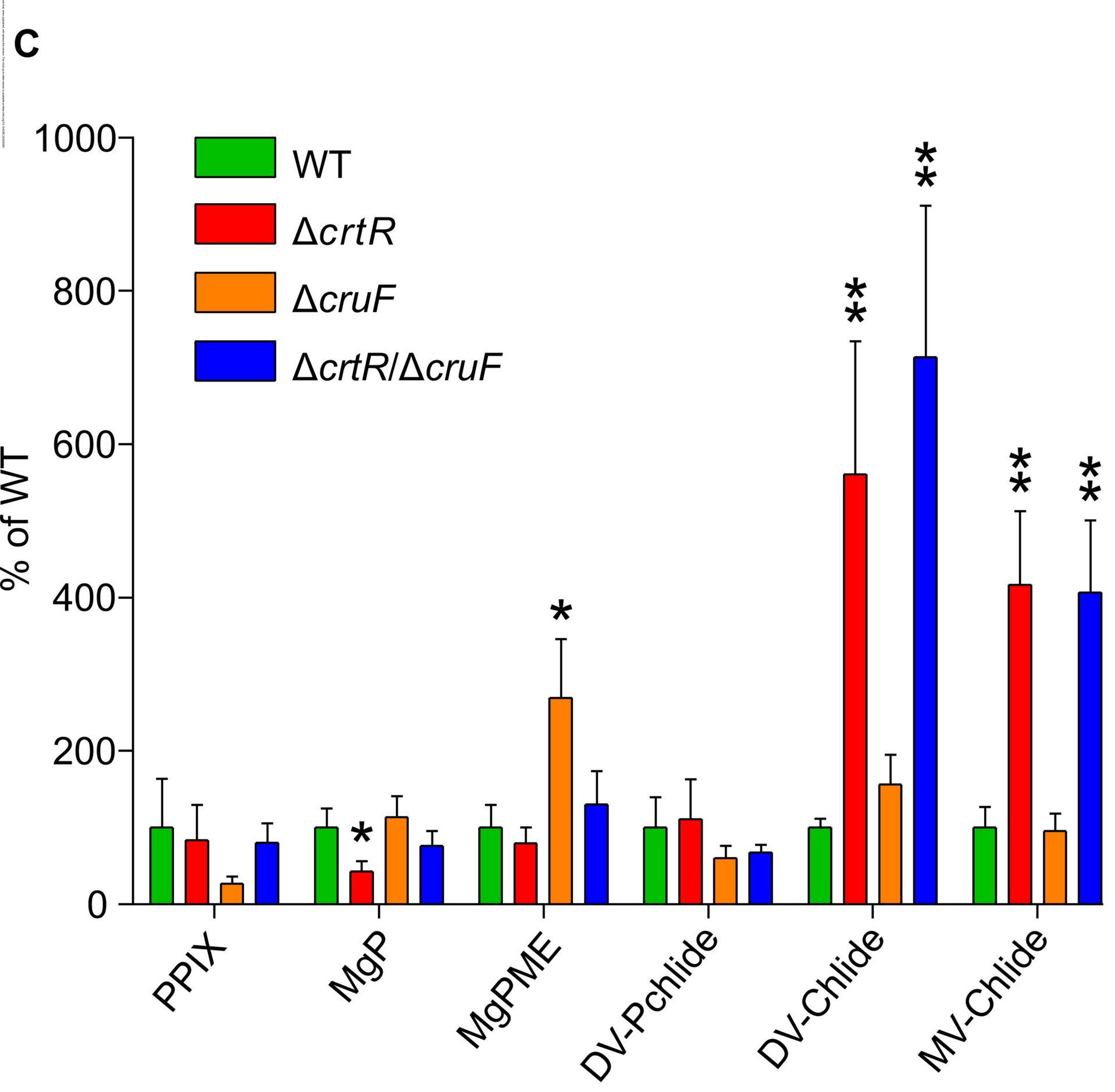
1000
800
600
400
200
0
% of WT
WT
ΔcrtR
ΔcruF
ΔcrtR/ΔcruF
*
**
PPIX
MgP
MgPME
DV-Pchlide
DV-Chlide
MV-Chlide